U.PORTO
FACULDADE DE CIÊNCIAS
UNIVERSIDADE DO PORTO

MSc

MSc
2.º CICLO
FCUP
2021

U.PORTO

Can EE2 ameliorate cobalt-induced stress in tomato plants? The effect of these pollutants on tomato's heavy metal homeostasis, antioxidant metabolism and its xenome

David João Machado Correia

FC

Can EE2 ameliorate cobalt-induced stress in tomato plants? The effect of these pollutants on tomato's heavy metal homeostasis, antioxidant metabolism and its xenome

David João Machado Correia

Dissertação de Mestrado apresentada à
Faculdade de Ciências da Universidade do Porto em
Biologia Funcional e Biotecnologia de Plantas

2021

MSc

Can EE2 ameliorate cobalt-induced stress in tomato plants? The effect of these pollutants on tomato's heavy metal homeostasis, antioxidant metabolism and its xenome

David João Machado Correia

Mestrado em Biologia Funcional e Biotecnologia de Plantas

Departamento de Biologia

2021

Orientador

Jorge Teixeira, Professor Auxiliar, FCUP

Coorientador

Fernanda Fidalgo, Professora Associada com Agregação, FCUP

Todas as correções determinadas pelo júri, e só essas, foram efetuadas.

O Presidente do Júri,

Porto, _____/_____/_____

“*You cannot teach a man anything;*

you can only help him discover it in himself”

- **Galileo Galilei**

Data presented in the following scientific communication was used for the elaboration of this master dissertation:

- Correia, D., Fidalgo, F., Teixeira, J. (2021). Participation of the MT gene family in the protection against excess Co in tomato. 1st EUGLOH Plant Science Meeting. Porto, Portugal.

Agradecimentos

No fim da jornada que foi este ano, com todos os desvios e barreiras que foram surgindo, não posso deixar de agradecer a todos aqueles que me apoiaram e me ajudaram a chegar até ao fim.

Em primeiro lugar, quero agradecer ao meu orientador, Professor Doutor Jorge Teixeira, que me abriu portas desde o início para envergar por este caminho da investigação na área da fisiologia das plantas. Foi a forma como lecionava com entusiasmo que me cativou para olhar com mais atenção e perceber o quão fascinantes estes seres são. Obrigado por todo o apoio e pelo voto de confiança que me permitiram evoluir não só a nível profissional como a nível pessoal. Agradeço também à Professora Doutora Fernanda Fidalgo pela disponibilidade demonstrada e por todas as sugestões e concelhos que me ajudaram a guiar este projeto.

De seguida, agradeço a toda a equipa do Plant Stress Lab por me apoiarem sempre que precisei, por me ensinarem a trabalhar e por serem um exemplo a seguir. Obrigado, Maria, a minha "lab mom" com quem dei os primeiros passos no mundo da investigação e é para mim um símbolo de força. Obrigado, Cris, não só por toda a ajuda e disponibilidade, mas por seres como és. Admiro imenso o teu trabalho e postura de vida e tive muita sorte em te ter presente enquanto definia a minha imagem mental do que era ser um investigador. Obrigado, Bruno, por todo o apoio naqueles longos dias a quantificar atividades enzimáticas. Sem ti não teria conseguido. Obrigado aos alunos cujo percurso tive o prazer de poder ajudar a guiar. Ajudaram-me imenso a crescer profissionalmente e foram uma excelente companhia. Eduardo, Eduarda, João e Sofia, desejo-vos muita sorte e sucesso, seja qual for a área que escolham seguir. A todos os outros, gostaria de agradecer pelos sorrisos, pelas conversas, pelos conselhos e sugestões e pelo apoio incondicional demonstrado. Muito obrigado!

Claro que nada disto seria possível sem o apoio e força da amizade. Obrigado, Tânia, por me ouvires e ajudares sempre que precisei, pelas palavras, emoções e risos trocados, pela presença constante nos melhores e piores dias e pela companhia e empatia que tornaram os obstáculos suportáveis. Obrigado, Adriana, Cláudia e Jéssica por estarem sempre lá para mim e por me contagiarem com energia positiva quando mais precisava dela. Obrigado, Rafa, pela total disponibilidade e prontidão em ajudar-

me sempre que possível, mas acima de tudo, pelo suporte que me deste para crescer. Devo muito do meu crescimento a ti, e tu sabes disso. Obrigado, Pedro, por me ajudares a encontrar a minha força naqueles momentos de maior insegurança e por todo o apoio emocional. És, para mim, um ótimo modelo de biólogo e, acima de tudo, de alguém que trabalha no que gosta, que é verdadeiro a si mesmo e segue os seus sonhos. Foste uma fonte de inspiração e motivação para seguir em frente. Obrigado à Mariana, Paulo e Rita, pelos desabafos e conversas que me ajudaram a sentir que não estava só e pelos risos e fugas para comer bolo que vieram decorar com boas experiências este percurso. A todos os amigos não mencionados, agradeço por toda a empatia, companheirismo e suporte emocional que foram essenciais para manter a esperança.

Um agradecimento muito especial aos meus pais e familiares pelo amor incondicional que me fez nunca desistir. Por serem uma constante na minha vida que me traz paz e estabilidade. Sem vocês, nada disto seria possível. Muito obrigado!

Resumo

Com o aumento exponencial da população humana e das atividades necessárias para a sustentar, há uma pressão sem precedentes nos ecossistemas. A poluição ambiental é um dos muitos fatores que contribuem para este estado de deterioração, com os metais pesados e os produtos e derivados farmacêuticos pertencendo aos mais preocupantes poluentes. O cobalto (Co) é um elemento essencial para a vida dos animais e seres procariontes, sendo constituinte da vitamina B_{12}, mas ainda não foi determinada uma função fisiológica nas plantas superiores. Tal como os outros metais pesados, o Co demonstra ser tóxico a muito baixas concentrações. Devido ao uso irresponsável de fertilizantes e a descargas de efluentes, os seus níveis nos solos estão a aumentar. O 17 α-ethinylestradiol (EE2) é um estrogénio sintético, presente na maioria dos contracetivos orais modernos, e é considerado um contaminante de preocupação emergente. O seu uso a nível mundial, resistência à degradação e ineficaz remoção pelas estações de tratamento de águas residuais contribuem para o aumento dos níveis deste poluente detetados nos diversos ecossistemas, onde afeta os seres vivos a partir de concentrações na gama de 1 $ng.L^{-1}$. No entanto, este composto parece estimular as plantas quando aplicado em baixas concentrações. Dado que as culturas estão frequentemente expostas a múltiplos poluentes, este trabalho visa explorar as respostas do tomateiro (*Solanum lycopersicum* L.) ao Co e ao EE2, numa exposição individual e combinada, e averiguar se o EE2 atua de forma antagonista ao Co quanto aos sintomas de toxicidade. Para isso, as concentrações de trabalho para ambos os contaminantes foram primeiramente otimizadas, através de ensaios de germinação. De seguida, As respostas bioquímicas, moleculares e fisiológicas, com particular foco na homeostasia redox, sistema antioxidante (AOX) e mecanismos de destoxificação, foram comparadas em plantas expostas a Co (50 μM), EE2 (500 $ng.L^{-1}$) e a uma combinação destes, por 5 semanas. Os resultados demonstram que o Co provocou efeitos negativos na biometria e morfologia da planta, diminuindo a sua biomassa, induzindo clorose e manchas necróticas nas folhas e reduzindo a acumulação de amido. Para além disso, este metal levou a uma acumulação dos níveis de peróxido de hidrogénio (H_2O_2) e afetou o sistema AOX, diminuindo a atividade da superóxido dismutase (SOD) e aumentando os níveis de ascorbato (AsA). Quanto à acumulação de transcritos, a exposição a este metal pesado afetou a expressão dos genes que codificam as metalotioninas (MTs), fitoquelatina sintase (PCS), glutationa redutase (GR) plastidial, glutationa S-transferase

(GST) da classe tau e γ-glutamil-cisteína sintetase (γ-ECS). As plantas expostas ao EE2 apresentaram maiores caules, mas também um maior grau de peroxidação lipídica, depleção dos níveis de glutationa (GSH), inibição da atividade da peroxidase do ascorbato (APX) e da GR, aumento da atividade da GST e uma expressão alterada de alguns genes relacionados com a destoxificação. À primeira vista, dado que a exposição a ambos os poluentes levou a níveis de biometria das plantas semelhantes aos do controlo, o EE2 parece ter auxiliado a aumentar a tolerância destes organismos ao Co, tendo os níveis de AsA e GSH aumentado nesta situação, assim como a atividade da GST, o que sugere que foi esta a estratégia que permitiu às plantas apresentarem níveis de biometria semelhantes aos do CTL. No entanto, os seus mecanismos de resposta demonstraram que esta co-exposição agravou alguns dos parâmetros que foram induzidos pelo Co, como os níveis de H_2O_2, e inibiu a expressão de alguns genes relacionados com a destoxificação. Este trabalho traz nova informação quanto aos efeitos do EE2 no sistema AOX e mecanismos de destoxificação das plantas e demonstra diferenças nas respostas destes organismos quando simultaneamente expostos ao Co e ao EE2, em comparação quando apenas expostos a um destes contaminantes. Para além disso, demonstra que genes codificantes das MTs e relacionados com as fitoquelatinas podem ter a sua transcrição influenciada por exposição da planta a estes contaminantes.

Palavras-chave

Farmacêuticos, *Solanum lycopersicum* L., xenobióticos, contaminação por metais pesados, metabolismo da glutationa, metalotioninas, co-exposição a contaminantes, estrogénios, 17 α-etinilestradiol.

Abstract

The exponential rise in human population, along with the activities needed to support it, put an unprecedented pressure on the ecosystems. Environmental pollution is one of the many factors which contribute to this deteriorating state, with heavy metals (HMs) and pharmaceuticals and their derivates being among the most concerning pollutants. Cobalt (Co) is an essential element for animals and prokaryotes, being part of vitamin B_{12}, but, in higher plants, a physiological function has yet to be determined. As other HMs, it induces signs of toxicity even at very low concentrations and, as a result of irresponsible use of fertilizers and wastewater discharge, its levels in the soil are increasing. 17 α-ethinylestradiol (EE2) is a synthetic estrogen, present in most modern oral contraceptive pills and is considered a contaminant of emerging concern. Its worldwide use, resistance to degradation and ineffective removal from wastewater treatment plants all contribute to greater levels being present in the ecosystems, where it can affect life at concentrations as low as 1 $ng.L^{-1}$. In plants, however, it appears this compound can have a stimulant role, when applied at low dosages. Since crops are very often exposed to more than one pollutant under field conditions, this study aimed at providing knowledge on how tomato plants (*Solanum lycopersicum* L.) respond to a Co and EE2 exposure, both individually and combined, and assess whether EE2 might act antagonistically to Co regarding toxicity symptoms. First, working concentrations for both contaminants were optimized, through germination assays. Then, the biochemical, molecular, and physiological responses were compared, particularly focusing on the redox homeostasis, antioxidant (AOX) system and detoxification mechanisms, in response to an exposure to 50 µM Co, 500 $ng.L^{-1}$ EE2, and the combination of both, for 5 weeks. The results revealed that the Co exposure led to harmful effects in the plant's biometry and morphology, reducing its biomass, inducing chlorosis and necrotic spots in the leaves, and impairing starch accumulation. Exposure to this HM also induced an accumulation of hydrogen peroxide (H_2O_2) and affected the AOX system, decreasing superoxide dismutase (SOD) activity and increasing ascorbate (AsA) levels. Regarding transcript accumulation, exposure to this HM affected metallothioneins (MTs), phytochelatin synthase (PCS), plastidial glutathione reductase (GR), tau class glutathione S-transferase (GST) and γ-glutamyl cysteine synthetase's (γ-ECS) expression. The treatment with EE2 increased shoot size but induced lipid peroxidation (LP), depleted glutathione (GSH) levels, inhibited ascorbate peroxidase (APX) and GR's activity, increased GST's activity, and

altered transcript accumulation for some detoxification-related genes. At first glance, in the coexposure, EE2 appeared to ameliorate the effects of Co, as the biometric values were similar to the control (CTL)'s, but the plants' response mechanisms demonstrated that, more often than not, the coexposure to these contaminants aggravated the plants' stress, increasing reactive oxygen species' levels, and inhibiting gene expression of detoxifying agents. Still, GSH and AsA levels were stimulated in this situation, which is most likely how the plants managed to revert to biometric levels close to those of the CTL. This research provided novel information concerning the effects of EE2 in plants' AOX system and detoxifying mechanisms and has evidenced differential responses from these organisms when exposed to both EE2 and Co, or to just one of these pollutants. Furthermore, it demonstrated that MTs- and PCs-related genes can have their transcription influenced by an exposure to these contaminants.

Keywords

Pharmaceuticals, *Solanum lycopersicum* L., xenobiotics, heavy metal contamination, glutathione metabolism, metallothionein, coexposure to contaminants, estrogens, 17 α-ethinylestradiol.

Table of Contents

List of Figures

List of Tables

Abbreviations, acronyms, and symbols

$^1O_2$ – singlet oxygen

aa – amino acid

Abs – absorbance

AOX – antioxidant

APX – ascorbate peroxidase

As – arsenic

AsA – ascorbate

BIP – 2,2'-bipyridine

BSA – bovine serum albumin

Car – carotenoids

CAT – catalase

Cd – cadmium

cDNA – complementary DNA

CDNB – 1-chloro-2,4-dinitrobenzene

CEC – contaminants of emerging concern

Chl – chlorophyll

Co – cobalt

$CoSO_4.7H_2O$ – cobalt (II) sulfate heptahydrate

Cr – chromium

CTL – control

Cu – Copper

cv. – cultivar

Cys – cysteine

d. w. – dry weight

ddH_2O – distilled and deionized water

DHA – dehydroascorbate

DHAR – dehydroascorbate reductase

DTNB – 5,5'-dithiobis (2-nitrobenzoic acid)

DTT – dithiothreitol

EDTA – ethylenediaminetetraacetic acid

E2 – 17β-estradiol

EE2 – 17α-ethinylestradiol

EF1 – Elongation Factor 1

f. w. – fresh weight

Fe – iron

Glu – glutamic acid

Gly – glycine

GPX – glutathione peroxidase

GR – glutathione reductase

GS – glutamine synthetase

GSH – glutathione

GSS – glutathione synthetase

GSSG – glutathione disulfide

GST – glutathione S-transferase

H_2O_2 – hydrogen peroxide

HEPES – (4-(2-hydroxyethyl)-1-piperazineethanesulfonic acid)

HM – heavy metal

HS – Hoagland's nutrient solution

I_2 – iodine

KI – potassium iodide

LP – lipid peroxidation

Lut – lutein

LWC – leaf water content

MDA – malondialdehyde

MT – metallothionein

N_2 – nitrogen

NaN_3 – sodium azide

NBT – nitroblue tetrazolium

NEM – N-ethylmaleimide

Ni – nickel

$O_2^{\bullet-}$ –superoxide anion radical

$^{\bullet}OH$ –hydroxyl radical

Pb – lead

PC – phytochelatin

PCR – polymerase chain reaction

PCS – phytochelatin synthase

PK – potassium phosphate buffer

PPCP – pharmaceuticals and personal care products

Pro – proline

PVPP – polyvinylpolypyrrolidone

ROS – reactive oxygen species

RT – room temperature

RT-PCR – reverse transcriptase PCR

SB – sodium boric acid

SD – standard deviation

SN – supernatant

SOD – superoxide dismutase

SH – sulfhydryl group

TBA – thiobarbituric acid

TCA – trichloroacetic acid

WWTP – wastewater treatment plants

Zn – zinc

β-car – *β*-carotene

γ-EC – γ-glutamylcysteine

γ-ECS – γ-glutamyl-cysteinyl synthetase

ε – molar extinction coefficient

1. Introduction

1.1. Environmental contamination

With the exponential rise in world population, accompanied with an ever-increasing industrialization, urbanization and intensive agriculture, there is an unprecedented pressure on the ecosystems. The widespread accumulation of pollutants and depletion of natural resources that ensue this reality are causing serious disturbances in the biosphere, including threats to human health (Panagos et al., 2013). Among the pollutants of higher concerns nowadays are heavy metals (HMs) and pharmaceuticals and their derivates.

1.1.1. Heavy metals (HMs)

Although "heavy metals" is not a standardized term, there is a consensus that it comprises metals, semimetals and metalloids with a density five times higher than water's and a potential for toxicity, even at low concentrations (Nagajyoti et al., 2010). Heavy metals include arsenic (As), cadmium (Cd), cobalt (Co), chromium (Cr), iron (Fe), nickel (Ni), lead (Pb) and zinc (Zn), amongst others. Even though these elements are naturally present in the Earth's crust and arise due to weathering processes and geological activity, anthropogenic-mediated addition of HMs to the environment (namely atmospheric deposition, waste disposal and burning, urban effluents, usage of wastewater in agriculture, etc.) is almost three times higher as compared to the natural factors (Mahey et al., 2020). This leads to much greater levels than expected, inducing toxicological risks in multiple systems. In fact, HMs are the main pollutants causing soil and groundwater contamination, accounting for about 35 % and 31 % of it, respectively (Panagos et al., 2013), with more than 5 million sites reported to be polluted by HMs (Emamverdian et al., 2015). Furthermore, it has been recognized that anthropogenic released metals are more easily available than those coming from geogenic sources (Bakshi et al., 2018).

Once present in the soil, they tend to accumulate and persist for a long duration of time, since they are not oxidized by microbes (Wuana and Okieimen, 2011). Some HMs have important roles on soil composition and nutrient cycles, even being considered as micronutrients for a healthy plant development and growth, such as Zn and Fe. In the plant, they can play a variety of roles, whether it is integrating enzyme composition,

acting as cofactors for various reactions, or even being involved in the redox system. Others, like As and Cd, are not known to perform any role in plant physiology. In both cases, however, concentrations higher than the associated threshold result in toxicity. Naturally, this threshold varies with the plant species, HM itself, soil properties and the environmental conditions that may compromise plants' ability to cope with the HM (Nagajyoti et al., 2010).

Plants growing at contaminated sites take up these HMs from affected soil–water and keep on accumulating them, eventually exceeding the threshold. In plant tissues, these pollutants can have deleterious effects in various mechanisms, unbalancing the cellular homeostasis and inducing stress. The most common way for this to happen is by an overproduction of reactive oxygen species (ROS) through the Haber-Weiss and Fenton reactions. The HMs capable of inducing this reaction, such as Co, Cr and Fe, are considered redox-active metals. The other group, non-redox active metals, like Cd, Ni and Zn, inflict oxidative stress in an indirect manner, including glutathione (GSH) depletion, antioxidant enzyme inhibition, binding to sulfhydryl (-SH) groups of proteins, among others.

1.1.1.1. Cobalt (Co)

Co is a naturally occurring element which is widely distributed in rocks and soils, where it is usually found as Co^{2+} (Gál et al., 2008). It is known to be an essential element for animals and prokaryotes and considered "beneficial" for legumes, since it is essential for several enzymes in nitrogen-fixing microorganisms such as *Rhizobium* and cyanobacteria, being a component of cobalamin (vitamin B_{12}) (Woodard et al., 2003). However, a physiological function for it in higher plants has not been determined so far (Wang et al., 2020).

Co is used in large quantities in the production of high-grade steels and alloys, and in smaller quantities as a drying agent in paints, varnishes, enamels and inks, as a pigment or as glass decolorizer, and as a catalyst in the petroleum industry (Adriano, 2013). Industries related to e-waste processing also utilize Co and have been found to release it above legal threshold levels (Nnorom and Osibanjo, 2009). As is the case for all HMs, Co cannot be chemically or biologically degraded and is, therefore, very difficult to remove from soils (Bakkaus et al., 2005) and other environmental matrices. The average Co content in the continental crust is 18 $mg.kg^{-1}$. However, depending on the parent rock

material, Co concentrations in soil can vary greatly: from 50–150 mg $Co.kg^{-1}$ in basic and ultrabasic rocks (with high contents of Fe- and Mn-rich minerals), to less than 1 mg $Co.kg^{-1}$ in sandstones and sands (Blume et al., 2010). Furthermore, Co content in wastewater has been reported to be above the permissible limit for crop irrigation (0.05 $mg.L^{-1}$) set by FAO (Pescod, 1992; Oladeji and Saeed, 2015).

As a result of the irresponsible use of fertilizers, wastewater discharge and increased mining activities, Co levels in soil have increased over the years (Mahey et al., 2020). Although Co is beneficial and even necessary for many organisms at the right concentrations, higher levels in soils induce toxicity symptoms in plants, at both morphological and physiological levels. For example, exposure of grown tomato plants to 0.5 mM Co (through sand medium) for 3 days led to the appearance of chlorosis on young leaves (followed by necrosis and withering), restricted the biomass, diminished the levels of chlorophyll (Chl) a and b and starch, and inhibited the activity of catalase (CAT; EC 1.11.1.6) (Gopal et al., 2003). Similarly, exposing tomato seedlings to 50 µM Co for 29 days (in moistened vermiculite and sand) reduced their biomass and induced leaf chlorosis (Bakkaus et al., 2005). Moreover, mustard (*Brassica juncea* L.) seedlings treated with 100 µM Co (hydroponic culture) for 8 days, showed significantly increased ascorbate (AsA), dehydroascorbate (DHA), GSH and oxidized glutathione (GSSG) contents in the leaves, as well as hydrogen peroxide (H_2O_2) levels, while superoxide dismutase (SOD; EC 1.15.1.1) and CAT's activities decreased and dehydroascorbate reductase (DHAR; EC 1.8.5.1) and glutathione reductase (GR; EC 1.6.4.2)'s activities increased (Karuppanapandian and Kim, 2013).

1.1.2. Pharmaceuticals

The term "contaminants of emerging concern" (CEC) refers to naturally occurring or manmade chemicals which have now been discovered (or are suspected) to be present in various environmental matrices and whose toxicity or persistence are likely to significantly disturb the metabolism of a living being (Sauvé and Desrosiers, 2014).

One of the most representative classes of CECs is that of pharmaceuticals and personal care products (PPCPs). With the advancements in medicine, the global use of pharmaceutical drugs has progressively increased. This myriad of compounds serve many purposes, namely as analgesics, antipyretics, antibiotics, antiseptics, hormone replacements, contraceptives, statins, mood stabilizers, antidepressants, and

cytostatics (Sadutto et al., 2021). After being consumed, either by humans or animals, some drugs are metabolized while others remain unchanged, before being excreted from the organism through the urinary and/or digestive tract (Monteiro and Boxall, 2010).

In general, the main established sources of pharmaceuticals in the environment are the following: effluents from manufacturing sites; hospital and human waste, including incorrect disposal of medicines; excretion by livestock treated with antibiotics, growth promoting agents and other formulations; the incomplete removal of many drugs in the wastewater treatment plants (WWTPs); runoff from agricultural fields fertilized with treated sewage sludge (Rzymski et al., 2017).

Depending on properties such as polarity, water solubility and persistence, some of these compounds may not be completely eliminated or transformed during sewage treatment in WWTPs (Monteiro and Boxall, 2010).

Even though PPCPs have long been released in the environment, what got them to become a widely acknowledged topic of concern derives from the development of analytical detection methods that made their ubiquity noticeable, and from the fact that their adverse environmental effects have recently been recognized (Erickson, 2002; Cardoso et al., 2014; Zenker et al., 2014; Soares et al., 2016; Martins et al., 2020).

1.1.2.1. 17 α-ethinylestradiol (EE2)

17 α-ethinylestradiol (EE2) is a synthetic analog of the naturally occurring 17β-estradiol (E2) and it is used in almost all modern formulations of combined oral contraceptive pills, being one of the most common medications (Aris et al., 2014). Its high resistance to degradation and greater oral bioavailability in the human body is one of its features that makes it useful in contraceptives. However, it also turns EE2 into a troubling contaminant.

The world's human population discharges approximately 700 $kg.year^{-1}$ of EE2, solely from birth control pill practices. Besides, EE2 is also used as medicine, meaning this value is possibly much lower than the actual emissions. Moreover, livestock practices, where EE2 is used to improve productivity and treat certain diseases (Gadd et al., 2010), also lead to substantial discharge values of this drug, ranging 80,000 $kg.year^{-1}$ (**Adeel et al.**, 2017). This hormone penetrates the surface and ground water systems through ineffective removal from WWTPs (Larcher and Yargeau, 2013), septic systems, and

through agricultural runoff, when sewage and manure are used as fertilizer (**Arnon et al.**, 2008), contaminating aquatic ecosystems worldwide (Dussault et al., 2009; Montagner and Jardim, 2011; Almeida et al., 2020). In aquatic systems, it can affect the endocrine systems of organisms in concentration levels as low as a nanogram per liter ($ng.L^{-1}$) (Ebele et al., 2017), being very toxic to a large number of exposed organisms (Saaristo et al., 2009; Dzieweczynski et al., 2014).

Due to the steady demand growth for this drug, an irregular distribution pattern has been found (Wang et al., 2018), but some of the most polluted rivers have been reported with levels from 17 to 4,390 $ng.L^{-1}$ (Montagner and Jardim, 2011). These higher levels are most likely linked to hot spot areas, namely those adjacent to agricultural and animal farms. Furthermore, with the increase in drought episodes connected with climate change (Nguyen et al., 2016), these levels may increase. For example, in the Douro river, in Portugal, the detected values were much higher in a year of particular drought, becoming extremely hazardous for the aquatic life (Ribeiro et al., 2009). Due to its hydrophobic properties, EE2 can concentrate in sediments (Lima et al., 2011), reaching concentrations up to 1000 times higher than in the overlying water column, which indicates that sediment may act as a sink and long-term accumulated source of this compound in aquatic systems. EE2 levels in sediments can also vary. Most detected values are between 0.1 and 5 $ng.g^{-1}$ (Aris et al., 2014), but much higher concentrations, reaching over 200 $ng.g^{-1}$, have been detected (Salgado et al., 2010; Froehner et al., 2012).

Although there has been much research conducted regarding the toxicity of this pollutant in animals (especially aquatic species), its effects on plants are still not well understood. Interestingly, the presence of estrogens and estrogenic activity in plants was discovered almost a hundred years ago. Some research suggests that the hormones regulating reproduction in animals have their phylogenetic origin in more primitive multicellular organisms [see Tarkowská (2019) and references therein]. Interestingly, E2 has been found to be naturally present in plant tissues, namely in female flowers (Simons and Grinwich, 1989), having specific binding sites within the cells (in the membranes and cytosol) (Janeczko et al., 2008) and playing an active role in processes such as germination (Speranza et al., 2011). In fact, its biosynthesis has previously been detected in *Phaseolus vulgaris* L. tissues, like in the seeds (Young et al., 1977). This implies that these plants would have the necessary mechanisms to regulate the internal

levels of this hormone, controlling its synthesis, conjugation, and degradation. Furthermore, there is a structural and functional resemblance between E2 and phytoestrogens, with a link to brassinosteroids (Janeczko and Skoczowski, 2005).

The synthetic EE2, due to its proximity to the natural E2, may also be recognized in plant tissues. Actually, at lower concentrations, EE2 reduced lipid peroxidation (LP) and H_2O_2 levels, while still increasing antioxidant (AOX) enzymes' activities (Erdal, 2009), suggesting a beneficial effect of this hormone in plants. Furthermore, numerous reports have shown that estrogens can alleviate some symptoms associated with several stresses, including HM induced stress (Erdal and Dumlupinar, 2011; Erdal, 2012; Genişel et al., 2015). Moreover, EE2 can enhance photosynthetic pigments and increase root growth and shoot biomass (Adeel et al., 2018). These differences may be due to a hermetic effect, where a low concentration of a toxic pollutant activates the plant's defense mechanisms, since, at higher concentrations, EE2 acts as a stressor on plant physiology, increasing LP and H_2O_2 levels (Christou et al., 2016) and increasing some AOX enzymes' activities, such as CAT, SOD and ascorbate peroxidase (APX; EC 1.11.1.11) (Adeel et al., 2018). Still, nonlinear relationships have been found in EE2 studies, making it a challenge when studying this hormone's effects on plants (Aris et al., 2014).

1.2. Research on coexposure to contaminants

In the last decades, most evaluations of the physiological effects of pollutants on plants have been studied only in single exposure approaches, while actual cases of contamination involving soils and plants implicate multiple pollutants. Soils are commonly contaminated by several pollutants simultaneously, mostly due to being simultaneously released and to the increasing re-utilization of sewage sludge and wastewater irrigation practices (Ye et al., 2017). In such circumstances, they can interact in a synergistic, additive, or antagonistic way in plants (Chaoui and El Ferjani, 2013). In fact, several studies have shown the potential of cotreatments to increase resistance in plants to a wide spectrum of stresses, activating distinct molecular, biochemical, and physiological processes than in plants exposed to one single abiotic stress (Mittler, 2006; Suzuki et al., 2014; De La Torre Roche et al., 2018; Liao et al., 2021).

1.3. Plant defense systems against pollutants

1.3.1. The plant's AOX system and redox homeostasis

ROS are partially reduced or excited forms of atmospheric oxygen (O_2), namely H_2O_2, singlet oxygen ($^1O_2$) and the radicals superoxide anion ($O_2^{\bullet-}$) and hydroxyl ($^{\bullet}OH$). ROS regulate plant growth and development and their levels are controlled by a balance between production and breakdown, which is achieved by a highly complex AOX system (Noctor et al., 2018). Under stress conditions, the production of ROS exceeds their scavenging mechanisms, leading to overproduction episodes. This state is called "oxidative stress" and is extremely harmful to organisms due to the disruption of cellular homeostasis. Oxidative stress may induce LP, protein oxidation, nucleic acid damage, enzyme inhibition, activation of programmed cell death and eventually cell death (Sharma et al., 2012).

The AOX system in plants is comprised of enzymatic and non-enzymatic components. The enzymatic elements of the AOX machinery include, amongst others, SOD, CAT, APX, monodehydroascorbate reductase (MDHAR; EC 1.6.5.4), DHAR and GR. Together, they maintain the redox homeostasis of the cell, as represented in Figure 1.

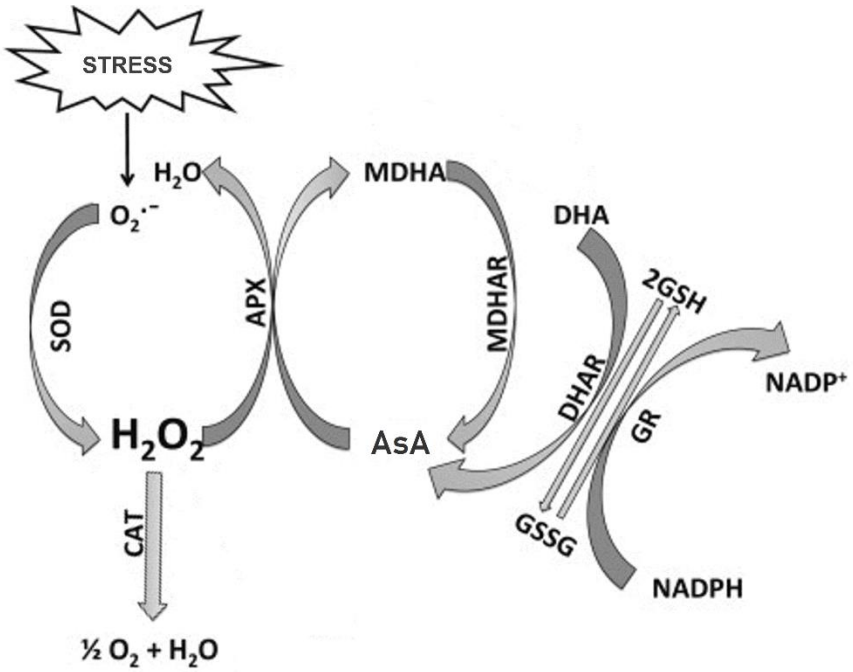

Figure 1 - AOX defense mechanism (AsA-GSH cycle). Adapted from (Gill and Tuteja, 2010).

The non-enzymatic AOXs form the other half of the AOX machinery. These include molecules like AsA, GSH, carotenoids (Car), phenolics, and proline (Pro), which not only play a protective role in different components of the cell, but also help to regulate plant growth and development via cellular processes like mitosis, cell elongation, senescence and apoptosis (de Pinto and De Gara, 2004).

AsA is the most abundant water-soluble redox compound in plants (Ishikawa and Shigeoka, 2008) and the majority of it originates from the Smirnoff-Wheeler pathway, catalyzed in the mitochondria, while the remaining is generated from D-galacturonic acid (Das and Roychoudhury, 2014). Its powerful AOX role in plant cells stems from its ability to donate electrons to a wide range of enzymatic and non-enzymatic reactions, and from the fact that its oxidized form is non-toxic. Besides being a vital part of the AsA-GSH cycle, it can also reduce ROS levels directly, repairing oxidized molecules (Sharma et al., 2012).

Well known for its osmoprotection, protein stabilization, LP inhibition and ROS quenching properties (Gill and Tuteja, 2010) that help to mitigate oxidative stress, Pro is an amino acid (aa) that is also directly involved in alleviating HM stress, acting as a chelator itself (Farago and Mullen, 1979; Sharma et al., 1998) and facilitating phytochelatins (PCs) formation (Siripornadulsil et al., 2002; Hayat et al., 2012). Furthermore, Pro levels seem to regulate the NADP+/NADPH ratio, which is important to maintain the reduced state of both AsA and GSH (Hare and Cress, 1997).

The role of GSH in the AOX system is presented in the next section.

1.3.2. HM detoxification pathways

A major strategy for detoxifying HMs is the synthesis of specific low molecular weight chelators, which prevent the binding of HMs to physiologically important proteins and facilitate their transport to vacuoles. These chelators include Pro (introduced in the previous section), GSH, PCs and metallothioneins (MTs).

1.3.2.1. Glutathione (GSH) metabolism

GSH is a low weight water-soluble tripeptide (γ-glutamyl-cysteinyl-glycine; γ-Glu-Cys-Gly) with a -SH group as the main chemically reactive group regarding its biological and biochemical functions (Hasanuzzaman et al., 2017). It is widely distributed in most plant tissues and has numerous functions in plants, being indispensable for their

survival (Tausz et al., 2004). The major processes for GSH synthesis occur in the chloroplast and consist of a two-step reaction (Hasanuzzaman et al., 2017). The first and limiting step is catalyzed by the enzyme γ-glutamyl cysteine synthetase (γ-ECS; EC 6.3.2.2) at the expense of ATP. It bonds cysteine (Cys) to glutamic acid (Glu), forming γ-glutamylcysteine (γ-EC). In the second step, glutathione synthetase (GSS, EC 6.3.2.3) catalyzes the ATP-dependent linkage between γ-EC and glycine (Gly), forming the final GSH product.

When the plant is under adverse or stress conditions, this reduced GSH is quickly converted into GSSG, mitigating (directly or indirectly) the oxidative stress induced by ROS. The balanced state of GSH/GSSG is maintained by the activities of two enzymes: GR and glutathione peroxidase (GPX; EC 1.11.1.7). The NADPH-dependent GR returns the oxidized GSSG to its original reduced state (GSH); whereas GPX catalyzes the opposite reaction (Noctor et al., 2012). Alternatively, GSH can play another role in detoxification of xenobiotics, via a glutathione-S-transferase (GST; EC 2.5.1.18)-mediated conjugation (Hasanuzzaman et al., 2017). GSTs are a heterogeneous superfamily with several classes, with GSTU (tau) class being one of the bigger classes present in plants (Labrou et al., 2015). They are a key component of plants' xenome, which is constituted by the members of the detoxification pathways in the cell (Labrou et al., 2015).

Another major function of GSH is the formation of PCs, that bind HMs for safe transport and sequestration in the vacuole (Yadav, 2010). They are a family of peptides with the general structure $(\gamma\text{-Glu-Cys})_n\text{-Gly}$, where *n* can range from 2 to 11. They are synthesized from GSH by phytochelatin synthase (PCS; EC 2.3.2.15). PCS's coding gene is constitutively expressed but the enzyme requires post-translational activation by metal(loid)s, (Hasanuzzaman et al., 2017). The PCs then bind to the HM ions, originating complexes that are subsequently sequestered in the vacuole, protecting the rest of the cell from HM toxicity (Anjum et al., 2015).

1.3.2.2. Metallothioneins (MTs)

MTs are low molecular weight Cys-rich proteins that present a high affinity for metal ions. This metal-binding capability is possible because the -SH groups of their Cys residues react with these metals, forming complexes that can then be sequestered in separate compartments, such as the vacuole, protecting the rest of the cell from toxicity (Roosens

et al., 2004). MTs are present in most living beings (Cobbett and Goldsbrough, 2002; Anjum et al., 2015), and have been studied in animals for over 60 years (Margoshes and Vallee, 1957). In plants, however, the MTs research field is still a recent one (Freisinger, 2011).

Their concrete functions in plants are not yet fully understood (Yang et al., 2009), however, given their metal-binding properties, their main role is to maintain the homeostasis of essential metals, like copper (Cu) and Zn, at micronutrient levels (Ren et al., 2012; R. Benatti et al., 2014), but also to detoxify non-essential toxic metals, such as Cd and As (Merrifield et al., 2004; Zimeri et al., 2005). Moreover, MTs appear to have additional roles on various other stress responses and physiological processes, namely protection against oxidative stress (Akashi et al., 2004; Hassinen et al., 2011) and seed germination (Brkljačić et al., 2004).

Unlike in other organisms, plant MTs have a higher level of variability in terms of size and aa composition. Each one has a characteristic number and pattern of Cys residues, which makes it possible to organize plant MTs into four groups, named MT1 to MT4 (Leszczyszyn et al., 2013). MT1, MT2 and MT3 have a similar organization, with two Cys-rich regions – the conserved C-terminal and the N-terminal, specific for each type – separated by a spacer region of approximately 40 aa. This region does not contain Cys but includes aromatic aa in its composition. Contrastingly, MT4 have three Cys-rich regions separated by spacer regions of 10 to 15 aa without neither Cys nor aromatic aa (Cobbett and Goldsbrough, 2002; Joshi et al., 2016).

An additional distinguishing factor between the four MT types is the distribution patterns of tissue specific gene expression for each MT. MT1's gene is highly expressed in roots, MT2's in shoots, MT3's in ripening fruits and leaves (Yang et al., 2009; Hassinen et al., 2011) and MT4's mainly in embryo tissues, seeds and reproductive tissues, although its expression has already been detected in different plant locations (Ren et al., 2012). This differential expression on a tissue level can indicate that each of these types of proteins performs specific functions (Leszczyszyn et al., 2013).

1.4. *Solanum lycopersicum* L. as a model species

Tomato plant (*Solanum lycopersicum* L.) is one of the most important horticultural crops in the world (Anwar et al., 2019). In Portugal, one of the biggest tomato producers in Europe, over 1,800,000 t are produced each year (Caldeira, 2019). Recently, it has

become an established model system for agronomically important traits that cannot be studied using other model plant systems (Kimura and Sinha, 2008) and an excellent model for plant stress physiology studies (Chaturvedi et al., 2018; Soares et al., 2019), as it has a relatively short life cycle, is not photoperiod dependent, has self-fertility and homozygosity, has its genome fully sequenced and is easy to manipulate (Gerszberg et al., 2015; Martins et al., 2020). Moreover, the tomato plant belongs to the extremely large Solanaceae family, meaning that knowledge obtained from studies conducted on tomato can easily be applied to these plants.

1.5. Objectives

Considering the increasing levels of HMs and pharmaceutical contaminants detected in water bodies, soils, plants and even animals, there is a pressing necessity to better understand these pollutants' modes of action, effects, and interactions. Furthermore, in the current climate change scenario — which aggravates the necessity of irrigation — the likelihood of crops being exposed to these compounds simultaneously is increased. Since crops are one of the most important components of our diet and vegetables are the major source of human exposure to HMs (Khan et al., 2015), studies on these plants are crucial to understand how these pollutants may impact crop yield, what mechanisms plants use to tolerate their toxicity and how their negative effects can be mitigated. Thus, this work aims to study the effects of Co and EE2 on tomato plants, (both understudied topics) seeking to uncover the damage caused by these contaminants and to characterize which defenses are activated both in a single and combined exposure to them. Moreover, since EE2 has been linked to beneficial effects in plants and estrogens have been demonstrated to ameliorate HM-induced stress symptoms, the possible antagonistic effect between these pollutants and the consequent protective role of EE2 were also evaluated. For this, several parameters were assessed, regarding the plants' growth, development, physiology and gene expression patterns. These include biometry, starch accumulation, photosynthetic pigments content, oxidative stress status, AOX system' response and transcript accumulation for key genes involved in the plants' detoxification mechanisms.

2. Materials and Methods

2.1. Biological material

For the purposes of this study, *S. lycopersicum* L. cv. Moneymaker (a commercial tomato cultivar) seeds were acquired and surface-disinfected with a 5-min immersion in 70 % ethanol and a 3-min immersion in a solution containing 20 % (v/v) commercial bleach and 0.02 % (v/v) Tween-20, in constant agitation. Following this procedure, the seeds were repeatedly washed with distilled and deionized water (ddH_2O) (to ensure no lingering substances remained adhered to the seeds' coats) and dried on blotting paper before being used.

2.2. Optimization of Co and EE2 concentrations

In order to establish the working concentrations of Co and EE2, initial germination assays were conducted for each tested pollutant. A series of growing concentrations of Co, administered as cobalt (II) sulfate heptahydrate ($CoSO_4.7H_2O$), ranging from 0 to 500 µM, was applied to seeds, in a Petri dishes' germination assay (described ahead), giving rise to the following treatments: 0, 25, 50, 75, 100, 125, 250 and 500 µM. These concentrations were selected from previous papers (Gopal et al., 2003) and based on relevant concentrations previously reported in the environment (Lago-Vila et al., 2015; Oladeji and Saeed, 2015).

Similarly, the impacts of growing concentrations of EE2 of tomato seeds' germination and seedling growth were assessed. EE2 was purchased from Sigma-Aldrich® (E4876) (Steinheim, Germany) and the following concentrations were tested: 0, 100, 250, 500, 750 and 1000 $ng.L^{-1}$. These concentrations were selected taking into consideration the previously reported environmental levels (Ribeiro et al., 2009; Salgado et al., 2010). An additional test was conducted, where the seeds were exposed to both the selected cobalt concentration (50 µM) and three EE2 concentrations (100, 500 and 1000 $ng.L^{-1}$) simultaneously. This would provide a first insight on the response of tomato plants to both these contaminants and allow for a selection of the concentrations to be used in the rest of the work.

2.2.1. Germination assays

In these assays, seeds (n = 10) were distributed in sterile Petri dishes (10 cm diameter) containing a solidified medium consisting of 0.5x modified Hoagland's nutrient solution (HS) (Taiz et al., 2015) supplemented with the respective pollutant's concentrations (described above) and 0.625 % (w/v) agar. Triplicates were made for each treatment. Subsequently, these Petri dishes were stored at 4 ºC and in the dark during 48 h to break seed dormancy and synchronize germination (stratification), and afterwards they were placed in a growth chamber with controlled optimized conditions (16 h light/ 8 h dark; 25 ºC) and 120 $\mu mol.m^{-2}s^{-1}$ photosynthetically active radiation for 5 days. Following this period, the germination rate was registered, and the grown plantlets were evaluated regarding their hypocotyl and main root size, as well as total fresh weight.

2.3. Growth trial

After optimizing the concentrations of Co and EE2, the main growth trial was performed by exposing tomato plants to 50 µM Co and/or 500 $ng.L^{-1}$ EE2. For this purpose, seeds were germinated *in vitro* as described above (without any pollutant). After 5 days, seedlings were transferred to opaque plastic pots filled with a 1:1 mixture of expanded vermiculite and perlite. Each pot housed three seedlings and a total of twelve pots were considered. For the first week, in order to acclimatize plantlets to the new conditions, all pots were irrigated only with half strength (0.5X) modified HS (Taiz et al., 2015). Afterwards, sets of three pots were randomly distributed and irrigated with different solutions, depending on the experimental group: CTL – 0.5x modified HS; Co – 0.5x modified HS supplemented with 50 µM Co; EE2 – 0.5X modified HS supplemented with 500 $ng.L^{-1}$ EE2; Co+EE2 – 0.5x modified HS supplemented with 50 µM Co and 500 $ng.L^{-1}$ EE2. Each group had its own tray below the pots, to allow a uniform bottom watering among the pots of each group. The nutritive medium was renewed when necessary. After five weeks, plants were removed from the pots, their roots washed with tap and then deionized water, and their biometrical data recovered. For this, shoots and roots were separated (division above the first lateral root) and the length and fresh weight of both portions of the plant were determined. The length of the aerial part was measured from the apical meristem to the separation site (mentioned above). As to the root length, the distance from the separation site to the tip of the main root was considered. Leaf samples from each plant were collected to evaluate relative leaf water content, pigments concentrations and starch accumulation. Afterwards, plants from each pot were grouped

together to be frozen and pulverized in liquid nitrogen (N_2). Aliquots were stored at -80 ºC until being used for biochemical and molecular assays.

2.4. Leaf physiology parameters

2.4.1. Leaf Water Content (LWC)

For estimating the leaf water content (LWC), foliar disks of 1 cm of diameter were extracted from the 3rd emergent leaf, lateral foliole, six disks per treatment, one disk per plant (two disks per pot), and rolled up into aluminum paper, containing a little hole to promote the air flow. Then, the disks were weighted in a high precision scale before and after being dried at 60 ºC until complete dehydration. The LWC was determined by calculating the difference between the fresh and dry weight (d. w.) of the disks and relative LWC was expressed in terms of percentage of the total fresh weight (f. w.).

2.4.2. Photosynthetic pigments evaluation

The quantification of total photosynthetic pigments was performed according to Tosin et al. (2021). Six disks of 1 cm of diameter were collected for each treatment, as described above but from the terminal foliole. Each disk was submerged in 5 mL of 80 % acetone (v/v) and stored at 4 ºC for approximately 24 h, until a complete bleaching of the disks was observed. After this period, extracts were centrifuged for 10 min at 2,000 *g* and the SN transferred to another tube, where the volume was adjusted to 5mL with 80 % (v/v) acetone, before measuring the absorbances (Abs) at 480 nm (Abs_{480}), 495 nm (Abs_{495}), 645 nm (Abs_{645}) and 655 nm (Abs_{655}). Following Bulda et al. (2008), equations (1) and (2), relative to Abs_{480} and Abs_{495}, were adopted to correct the influence of chlorophylls (Chl) and the remaining pigments in the extract's Abs. In these equations, Abs^{O}_{480} and Abs^{O}_{495} represent the original values for the Abs at 480 and 495 nm.

(1) $Abs_{480} = Abs^{O}_{480} – 0.566 \times Abs_{645} + 0.121 \times Abs_{655}$

(2) $Abs_{495} = Abs^{O}_{495} – 0.112 \times Abs_{645} – 0.0036 \times Abs_{655}$

The following equations, present in the same study, were then used to obtain the concentrations of each pigment (expressed in $mg.L^{-1}$) [(3) chlorophyl a (Chl_a), (4) chlorophyl b (Chl_b), (5) β-carotene (β-car), (6) lutein (Lut)]:

(3) $Chl_a = 19.00 \times Abs_{655} - 7.61 \times Abs_{645}$

(4) $Chl_b = 21.45 \times Abs_{645} - 5.92 \times Abs_{655}$

(5) β-car = 17.16 x Abs_{495} - 3.96 x Abs_{480}

(6) Lut = 11.51 x Abs_{480} - 20.61 x Abs_{495}

The content of each pigment studied was expressed in $mg.g^{-1}$ f. w..

2.4.3. Histochemical coloration of starch

In order to assess whether Co and/or EE2 had any impact on starch storage of tomato leaves, a histochemical coloration of the starch grains was performed. First, leaf discs of 1 cm diameter were collected from the terminal foliole of the 4th emergent leaf, four disks per treatment, each from a different plant. Then, the discs were boiled in 80 % (v/v) ethanol, to allow leaf bleaching, and submerged in ddH_2O water for 1 min, to allow tissue rehydration. Afterwards, the discs were incubated in a Lugol solution [2 mM iodide (I_2), 6mM potassium iodide (KI)] for 30 min in the dark, to stain the starch present in the tissues. Finally, the samples were briefly distained in distilled water and the results were visualized and captured with a personal photographic camera.

2.5. Analysis of biochemical parameters

2.5.1. Determination of lipid peroxidation (LP)

LP was evaluated as described by Heath and Packer (1968), by the quantification of malondialdehyde (MDA) levels, since it is an end product formed from polyunsaturated fatty acids peroxidation in the cells, allowing an indirect evaluation of membrane damage. Frozen aliquots of 200 mg were homogenized in 0.1 % (w/v) trichloroacetic acid (TCA) (1.5 mL for shoots and 1 mL for roots) in the Bead Mill Homogenizer BEAD RUPTOR 12 from Omni International Inc. (Dublin, Ireland), using 5 beads per tube, and a program with 3 homogenizing cycles of 20 s. To prevent sample overheating, the tubes were incubated on ice for 1 min between each cycle. Extracts were centrifuged during 5 min at 10,000 *g* (4 ºC). Afterwards, 600 µL of 0.5 % (w/v) thiobarbituric acid (TBA) in 20 % (w/v) TCA were added to 150 µL of recovered SN. For the blank measurement, homogenization solution was utilized instead of SN. Tubes containing this mixture were incubated at 95 ºC for 30 min, and subsequently cooled on ice for 10 min, before an 8-min centrifugation at 10,000 g. The Abs values of each sample were read at both 532 and 600 nm, the latter being subtracted to the first to remove the effects of non-specific turbidity. MDA content, expressed as $nmol.g^{-1}$ f. w., was determined applying the molar extinction coefficient (ε) of 155 mM^{-1} cm^{-1}.

2.5.2. Quantification of H_2O_2

The quantification of H_2O_2 levels was performed according to the procedures described by Alexieva et al. (2001), using the same SN obtained for the evaluation of LP, previously summarized. After centrifugation, 250 µL of the SN were added to 250 µL of 100 mM potassium phosphate (PK) buffer (pH 7.0) and 1 mL of 1 mM KI. A blank reaction was prepared, replacing the SN with 250 µL of 0.1 % (w/v) TCA. The tubes were incubated at room temperature (RT), for 1 h, in the dark. Subsequently, the Abs of each sample was recorded at 390 nm. The levels of H_2O_2 were quantified using the ε value of 0.28 $\mu M^{-1}cm^{-1}$ and expressed as nmol H_2O_2 g^{-1} f. w..

2.5.3. Quantification of non-enzymatic AOX metabolites

2.5.3.1. Determination of proline (Pro) levels

The Pro levels were evaluated according to Bates et al. (1973). Frozen samples of 200 mg were homogenized in 3 % (w/v) sulfosalicylic acid (1.5 mL for shoots and 1 mL for roots) in the BEAD RUPTOR 12, using 5 beads per tube, and a program with 3 homogenizing cycles of 20 s. To prevent sample overheating, the tubes were incubated on ice for 1 min between each cycle. Homogenates were then centrifuged at 16,000 *g* for 20 min (4 ºC). Afterwards, 200 µL of SN were mixed with 200 µL of glacial acetic acid and 200 µL of acid ninhydrin, followed by an incubation at 96 ºC for 1 h. After briefly cooling on ice, 1 mL of toluene was added to each sample and the mixture was vortexed for 15 seconds to separate a red upper phase (organic) from a whiteish lower phase (aqueous). The upper one was recovered, and its respective Abs read at 520 nm. Toluene was used as the blank. Pro concentration was estimated via a standard curve designed with increasing known Pro concentrations and results were expressed as $\mu g.g^{-1}$ f. w..

2.5.3.2. Quantification of reduced glutathione (GSH)

The levels of GSH were evaluated according to a protocol optimized by Soares et al. (2019), using the same SN as for the Pro quantification, described above. After centrifugation, 50 µL of SN were added to 200 µL of H_2O and 750 µL of a reaction mixture containing 100 mM PK buffer (pH 7.0), 1 mM ethylenediaminetetraacetic acid (EDTA) and 0.1 M 5,5'-dithiobis-(2-nitrobenzoic acid) (DTNB; Ellman's Reagent). Tubes were briefly vortexed and subsequently incubated at RT, in the dark, for 10 min. Afterwards,

the Abs was read at 412 nm and the levels of reduced GSH were calculated according to a standard curve, obtained with solutions of known concentration of reduced GSH. The results were expressed in μmol GSH g^{-1} f. w..

2.5.3.3. Quantification of ascorbate - reduced (AsA) and oxidized (dehydroascorbate – DHA) forms

Quantification of ascorbate was conducted by following the procedures described by Gillespie and Ainsworth (2007). For this assay, frozen aliquots of approximately 200 mg were homogenized in 6 % TCA (w/v) (1.5 mL for shoots and 1 mL for roots) at 4 ºC, in the BEAD RUPTOR 12, using 5 beads per tube, and a program with 3 homogenizing cycles of 20 s. To prevent sample overheating, the tubes were incubated on ice for 1 min between each cycle. Afterwards, homogenates were centrifuged at 15,000 *g* for 10 min (4 ºC), and the SN was collected to new tubes. At this point, two separate sets of reactions were assembled, one to quantify the levels of total ascorbate and a second one to quantify reduced ascorbate (AsA) levels. For total ascorbate quantification, 100 μL of SN were added to 50 μL of 75 mM PK buffer (pH 7.0) and 50 μL of 10 mM 1,4-dithiothreitol (DTT). DTT reduces DHA, turning all ascorbate present in the sample to AsA. This mixture was briefly vortexed and incubated at RT for 10 min. Subsequently, 50 μL of 0.5 % (w/v) N-ethylmaleimide (NEM) were added to remove excess active DTT, by blocking its sulfhydryl groups. To assess the levels of AsA, 100 μL of SN were mixed with 50 μL of 75 mM PK buffer (pH 7.0) and 100 μL of ddH_2O (to compensate for the volumes of DTT and NEM that had been added to the total ascorbate quantification tubes). Then, 750 μL of a reaction mixture containing 10 % (w/v) TCA, 43 % (v/v) H_3PO_4, 4 % (w/v) 2,2'-bipyridine (BIP) and 3 % (w/v) $FeCl_3$ were added to all tubes (for total ascorbate and AsA quantification). All samples were incubated at 37 ºC for 1 h. In this period, AsA reduced the Fe^{3+} ions from $FeCl_3$ to Fe^{2+}, which subsequently reacted with BIP, forming a complex with a characteristic Abs peak at 525 nm. This allows for an indirect AsA quantification. After incubation, the Abs were recorded at 525 nm (Fe^{2+}-BIP complex Abs peak). The concentrations of total and reduced AsA were calculated from a calibration curve previously prepared with solutions of known AsA concentration. The levels of oxidized ascorbate were estimated by subtracting the reduced portion from the total ascorbate pool. Results were expressed in μmol AsA (or DHA) g^{-1} f. w..

2.5.4. Extraction and quantification of soluble proteins

To quantify the levels of total soluble proteins, frozen samples were homogenized in an extraction buffer (1.5 mL for shoots and 1.2 mL for roots) consisting of: 100 mM PK buffer (pH 7.3), 1 mM EDTA, 8 % (v/v) glycerol; 1 mM phenylmethylsulphonyl fluoride (PMSF); 5 mM AsA; and 2 % (w/v) polyvinylpolypyrrolidone (PVPP). These constituents ensure protein stability and protection against proteases. Samples were homogenized in the BEAD RUPTOR 12, using 5 beads per tube and a program with 3 homogenizing cycles of 20 s. Between each cycle, a 1 min incubation of the tubes on ice was implemented, to prevent sample overheating. The extracts were then centrifuged at 16,000 *g* for 35 min (4 ºC), and the resulting SN was used to quantify the total soluble proteins, as well as to measure the activity of SOD, CAT, APX, DHAR, GR and GST (key enzymes in the plant's defense system against pollutants). Total soluble proteins quantification was performed according to Bradford (1976), by measuring the Abs at 595 nm. A calibration curve was assembled by utilizing standard samples of different known concentrations of bovine serum albumin (BSA). Results were expressed in mg protein g^{-1} f. w..

2.5.5. Determination of ROS-scavenging enzymatic activity

2.5.5.1. SOD activity assay

The total activity of SOD was quantified based on the spectrophotometric assay described by Donahue et al. (1997), which measures the inhibition of the photochemical reduction of nitroblue tetrazolium (NBT) to blue formazan. The protein extracts were complexed with 0.3 mM sodium azide (NaN_3; 1 µL NaN_3 per 30 µL of protein extract) to ensure peroxidase inhibition. A reaction mix was then prepared, consisting of 50 mM PK buffer (pH 7.8), 0.1 mM EDTA, 13 mM methionine and 75 µM NBT. An initial test was undertaken to ensure that the detected SOD activity was in the linear phase, so that the values could be compared between treatments. For this, several protein amounts (complexed with NaN_3 as previously described) were tested (following the procedures described ahead) and an optimal quantity was obtained. The volume of complexed extract containing the optimal amount of protein was mixed with 2.8 mL of the reaction mix, 30 µL of 2 µM riboflavin and 50 mM PK buffer (pH 7.8) to a final volume of 3 mL. The reaction started with the addition of riboflavin. Tubes were quickly shaken and incubated for 10 min at RT, under exposure to 6 fluorescent 8 W lamps, with constant rotation (to ensure an even exposure of the samples to the light). By exposing riboflavin

to this light in the presence of O_2, and having methionine as an electron donor, the superoxide anion (O_2^-) is formed. This ROS reduces NBT, forming blue formazan. A blank tube was prepared under the same conditions, replacing the protein extract with 100 mM PK buffer (pH 7.3). After this period, the Abs of all tubes, including the blank, was measured at 560 nm (blue formazan Abs detection peak), using the empty cuvette as the spectrophotometric blank. The higher the SOD activity, the lower the Abs obtained, since less O_2^- is available to reduce NBT to blue formazan. Therefore, enzyme activity was determined in terms of NBT reduction, following these calculations:

• % oxidized NBT = Abs (sample) / Abs (blank) x 100

• % NBT reduction = 100 - % oxidized NBT

The activity of SOD was expressed according to Beauchamp and Fridovich (1971) as units of SOD mg^{-1} protein, in which one unit of SOD corresponds to the amount of enzyme needed to inhibit the photochemical reduction of NBT by 50 %.

2.5.5.2. CAT activity assay

The activity of CAT was spectrophotometrically assayed following a procedure described by Soares et al. (2018), based on methods of Aebi (1984). This evaluation was performed in a 96-well UV microplate, in a final volume of 200 µL, in which 20 µL of protein extract were added to 160 µL of 50 mM PK buffer (pH 7.0) and 20 µL of 100 mM H_2O_2. After mixing for 5 s, the rate of H_2O_2 consumption was recorded in the Multiskan GO® spectrophotometer (Thermo Fisher Scientific) at 240 nm, every 5 s, for a total of 1 min and 30 s. The activity of CAT was calculated and expressed in terms of H_2O_2 consumption, considering an ε value of 39.4 mM^{-1} cm^{-1}, as nmol of H_2O_2 min^{-1} mg^{-1} of protein.

2.5.5.3. APX activity assay

Similarly to CAT's, the activity of APX was also assessed spectrophotometrically using Miltiskan GO® in a 96-well UV microplate, through the oxidation of AsA, following the methods of Murshed et al. (2008). In each well, 20 µL of protein extract were combined with 170 µL of 50 mM PK buffer (pH 7.0) supplemented with 0.6 mM AsA, and the reaction started upon adding 10 µL of 254 mM H_2O_2. After agitating for 5 s, the variations in Abs at 290 nm were recorded every 5 s, for a total of 1 min and 30 s. The total activity

of APX, measured by the potential to oxidize AsA into DHA, was calculated using an ε value of 0.49 mM^{-1} cm^{-1} and expressed in µmol of AsA min^{-1} mg^{-1} of protein.

2.5.5.4. DHAR activity assay

The activity of DHAR was assessed spectrophotometrically, as previously described, using Multiskan GO® in a 96-well UV microplate, through the GSH-dependent reduction of DHA, following the methods of Murshed et al. (2008). In each well, 20 µL of protein extract were combined with 170 µL of HEPES buffer 50 mM (pH 7), supplemented with EDTA 0.1 mM and GSH 2.5 mM, and the reaction started upon adding 10 µL of DHA 8 mM. After agitating for 5 s, the variations in Abs at 265 nm were recorded every 5 s, for a total of 1 min and 30 s. The total activity of DHAR, measured by the potential to reduce DHA into AsA, was calculated using an ε value of 14 mM^{-1} cm^{-1} and expressed in nmol AsA min^{-1} mg^{-1} protein.

2.5.5.5. GR activity assay

The activity of GR was assessed spectrophotometrically, as previously described, using Multiskan GO® in a 96-well UV microplate. following the methods of Murshed et al. (2008). In the microplate, the final volume of 200 µL contained 160 µL of 50 mM HEPES buffer (pH 8.0) supplemented with 0.5 mM EDTA and 0.25 mM NADPH, 30 µL of extract and 10 µL 20 mM GSSG. The reaction was initiated upon the addition of GSSG. After a 5 s agitation, the activity of GR was determined by monitoring the oxidation of NADPH at 340 nm for 1 min and 30 s. The activity was calculated using an ε value of 6.22 mM^{-1} cm^{-1} and expressed as µmol min^{-1} mg^{-1} protein.

2.5.6. Determination of GST activity

The activity of GST was assayed according to Teixeira et al. (2011). In order to determine GST's activity, 700 µL of 50 mM of phosphate buffer (pH 7.5), 100 µL of 1 mM chlorodinitrobenzene (CDNB), 100 µL of extract and 100 µL of 10 mM GSH (initiates the reaction) were pipetted into a cuvette and, after a brief shaking, the increase in the Abs (ΔAbs) was read at 340 nm for 2 min. So as to determine the non-enzymatic conjugation of CDNB to GSH, 100 µL of extract were substituted by 100 µL of extraction buffer. The latter ΔAbs 340 nm min^{-1} was subtracted to the first value to estimate the real GST activity using the ε value of 9.6 mM^{-1} cm^{-1} and results were expressed as µmol min^{-1} mg^{-1} protein.

2.6. Analysis of transcript accumulation patterns

2.6.1. RNA extraction and quantification

Total RNA from plant tissues was extracted with the phenolic solution NZYol® (NZYTech, Lda., Portugal), according to the supplied instructions. Frozen samples of roots and shoots (ca. 100 mg) were homogenized in 1 mL of NZYol® and were then centrifuged for 10 min at 12,000 *g* (4 ºC). The cleared homogenates were transferred to new sterile tubes and incubated for 5 min at RT. Then, 0.2 mL of chloroform were added, followed by 15 s of vigorous shaking to efficiently denature proteins and other cell constituents. After a 3 min RT incubation, samples were centrifuged at 12,000 *g* for 15 min (4 ºC), inducing a phase separation. Three distinct phases were obtained: a lower pale green, phenol-chloroform phase, an interphase with cell-debris and proteins, and a transparent aqueous upper phase, which contains the RNA. Carefully, the latter was recovered (without disturbance of the interphase) and transferred to new tubes, where the RNA was precipitated by adding 0.5 mL of chilled isopropanol. Following a 10 min incubation at RT, samples were centrifuged at 12,000 *g* for 10 min (4 ºC). After discarding the resulting SN, the pellet was washed by adding 1 mL of 75 % (v/v) ethanol, followed by a quick vortex and a 5 min centrifugation at 7,500 *g* (4 ºC). The final pellet was then air-dried and, once the ethanol had completely evaporated, was re-suspended in nuclease-free water.

RNA concentration was determined using a DS-11 Microvolume Abs Spectrophotometer from DeNovix® (DeNovix Inc., USA) at 260 nm, and results were expressed in terms of $ng.\mu L^{-1}$. RNA purity was evaluated by the calculation of the ratios Abs_{260}/Abs_{280} and Abs_{260}/Abs_{230}, which measure protein and phenolic contamination, respectively.

To assess RNA integrity, 300 ng of each RNA sample were analyzed by a 1 % (w/v) agarose gel electrophoresis in 1x sodium boric acid (SB) buffer, at 250 V and non-limiting amperage, and using Xpert Green DNA Stain (GRiSP, Portugal) to stain the nucleic acids. Samples considered acceptable in all evaluated parameters were stored at -80 ºC until further use.

2.6.2. Reverse Transcription (cDNA Synthesis)

To generate complementary DNA (cDNA) from the previously extracted RNA, reverse transcription reactions were performed with SuperScript™ IV VILO™ Master Mix kit, following the manufacturer's instructions (Invitrogen, USA). First, 2.5 µg of template RNA were transferred to chilled, sterile tubes, containing 4 µL of SuperScript™ IV VILO™ Master Mix (which includes dNTPs, oligo-dT and random primers) and nuclease-free water in a final volume of 20 µL. This reaction was gently mixed and incubated at 25 ºC for 10 min, enabling primer annealing. Subsequently, the reverse transcription took place at 50 ºC for 30 min. Finally, enzymes were inactivated with an 85 ºC incubation for 5 min. The synthesized cDNAs were stored at -20 ºC until future use.

2.6.3. Semi-quantitative polymerase chain reaction (PCR)

So as to assess the differences in the accumulation of the mRNAs coding for different enzymes involved in the GSH metabolism (PCS, plastidial GR, γ-ECS, and GSTU) as well for the four MTs (MT1, MT2, MT3 and MT4) after the different treatments with Co and EE2, semi-quantitative reverse-transcriptase PCRs (RT-PCRs) were performed. GSTU has many different genes, so the primers used were conserved to amplify all mRNAs from GSTU. All reactions consisted in: 5 µL of 2x Taq Master Mix (Bioron®), 0.4 µL of 10 µM forward and reverse primers, 0.5 µL cDNA obtained for each treatment and PCR water to a final volume of 10 µL. The reactions were performed in a MJ Mini thermocycler (Bio-Rad®) and the PCR conditions, as well as the primers' sequences and amplicon sizes, are described in Table 1. After the reaction, the amplification products were loaded on 1 % (w/v) agarose gels, following the same electrophoresis conditions described above. To ensure that differences observed are due to a differential gene expression, it was necessary to assure that an equal amount of cDNA was loaded for all samples. For this, the *Elongation Factor 1* (*EF1*), a housekeeping gene, was used as a reference to determine the volume of all treatments' amplicons to load (Løvdal and Lillo, 2009). In this sense, *EF1* amplicons for each treatment were loaded and the volumes which resulted in similar bands were utilized in the ensuing comparative quantifications. Gene Ruler 50 bp DNA Ladder (Thermo Fisher Scientific®) was used to verify the size of the amplified fragments. All images were captured and treated with GenoSmart2 (VWR, USA).

Table 1 – Specific primers for *EF1*, *MT1*, *MT2*, *MT3*, *MT4*, *GSTU*, *PCS*, *γ-ECS* and plastidial GR (GR_{plast}) used in PCR reactions, with respective expected amplicon sizes and programs used. F – Forward primer, R – Reverse primer

Gene	Accession number	Primer sequence	Amplicon size (bp)	Thermocycler program
EF1	X14449	F: 5' GGAACTTGAGAAGGAGCCTAAG 3' R: 5' CAACACCAACAGCAACAGTCT 3'	158	Lid 110 ºC 94 ºC – 2 ' 29 cycles of: 94 ºC – 30 '', 60 ºC – 30 '', 72 ºC – 45 '' 72 ºC – 5 '
MT1	Z68185	F: 5' GGAGGAAGCTGTAATTGTGG 3' R: 5' CCCCCTTCTGTAGCTTTCTC 3'	166	Lid 110 ºC 94 ºC – 2 ' 29 cycles of: 94 ºC – 30 '', 54 ºC – 30 '', 72 ºC – 45 '' 72 ºC – 5 '
MT2	L77963.2	F: 5' GCTGTGGAGGATGTGGTATG 3' R: 5' CCTTCTCCAGCTGCTTTCTC 3'	117	
MT3	FJ546424	F: 5' GGAAGGAGAGCCAATACGAC 3' R: 5' TGTTCTTCTGCTCCAACGTC 3'	78	
MT4	XM_004231052.3	F: 5' ATGAGAGGTGTGGTTGTCCTT 3' R: 5' CCGCACTTGCAGTTAGACTT 3'	180	
GSTU	—	F: 5' GGGAAACCAATTTGTGAATC 3' R: 5' GCGTTGGCTCTTTCATAAGG 3'	568	Lid 110 ºC 94 ºC – 2 ' 29 cycles of: 94 ºC – 30 '', 51 ºC – 30 '', 72 ºC – 90 '' 72 ºC – 10 '
PCS	XM_004247469	F: 5' CAGAATGGAACAATGGAAGG 3' R: 5' GCAAACTAAAAGGGAGGTG 3'	570	Lid 110 ºC 94 ºC – 2 ' 29 cycles of: 94 ºC – 30 '', 53 ºC – 30 '', 72 ºC – 45 '' 72 ºC – 5 '
γ-ECS	NM_001247081	F: 5' GAAACAGGGAAAGCAAAGC 3' R: 5' CATCAGCACCTCTCATTTCC 3'	725	Lid 110 ºC 94 ºC – 2 ' 29 cycles of: 94 ºC – 30 '', 51 ºC – 30 '', 72 ºC – 45 '' 72 ºC – 5 '
GR_{plast}	NM_001321393	F: 5' AAAGACCGAGGAGATTGTACG 3' R: 5´ CATTCCTCGCCATATAGAAGC 3'	322	Lid 110 ºC 94 ºC – 2 ' 29 cycles of: 94 ºC – 30 '', 57 ºC – 30 '', 72 ºC – 45 '' 72 ºC – 5 '

2.1. Statistical analysis

For every parameter, at least three biological replicates (n ≥ 3), with at least three technical replicates were used per assay. The results were expressed as mean ± standard deviation (SD). Significant differences were monitored through a one-way ANOVA followed by the appropriate multiple comparisons tests, in this case, either Dunnett or Tukey's. Since one-way ANOVA is considered a sufficiently robust statistical test (Zar, 1996), it was used instead of nonparametric statistical tests, even when ANOVA assumptions were not met. These analyses were performed using Prism® 8 (GraphPad Software Inc., USA), considering significant the differences at $p \leq 0.05$.

3. Results

3.1. Effects of Co and EE2 on tomato plants' biometry

3.1.1. Effects of increasing Co concentrations on seed germination and early development

In order to gain an insight into the effects of Co in the first life stages of the tomato plant, and to simultaneously select an appropriate concentration for the long-term exposure assay, an initial germination assay was conducted. Five days after seed germination, the biometric data of seedlings exposed to growing concentrations of Co was collected and analyzed. Regarding germination rate (Figure 2 A), seedling biomass (Figure 2 B) and hypocotyl length (Figure 2 D), there were no significant differences between each tested concentration and the CTL. However, there was a significant decrease in root length for all concentrations higher than 25 μM (37 %, 50 %, 56 %, 57 %, and 73 % for 50 μM, 75 μM, 100 μM, 125 μM and 250 μM, respectively), in relation to the CTL (Figure 2 C). This gradual decrease can be visualized in Figure 3.

To select the concentration to be used in the following assays, several principles had to be taken under consideration: 1) the Haber's rule (C x t = k), where the lethal concentration of a toxicant (C) and the exposure time (t) are inversely proportional (Connell et al., 2016). Therefore, in a prolonged exposure assay, lower concentrations are preferred to visualize differences between treatments without compromising viability. 2) several reports using different types of contaminants have shown that germination and early growth parameters can possibly remain unaffected due to a protective effect of the seed coat, even in high and usually toxic concentrations (Li et al., 2005; Akinci and Akinci, 2010; Wu et al., 2021). Taking these aspects into consideration, the lowest concentration to produce a significant negative effect in the seedlings' biometry (50 μM) was selected for the posterior assays.

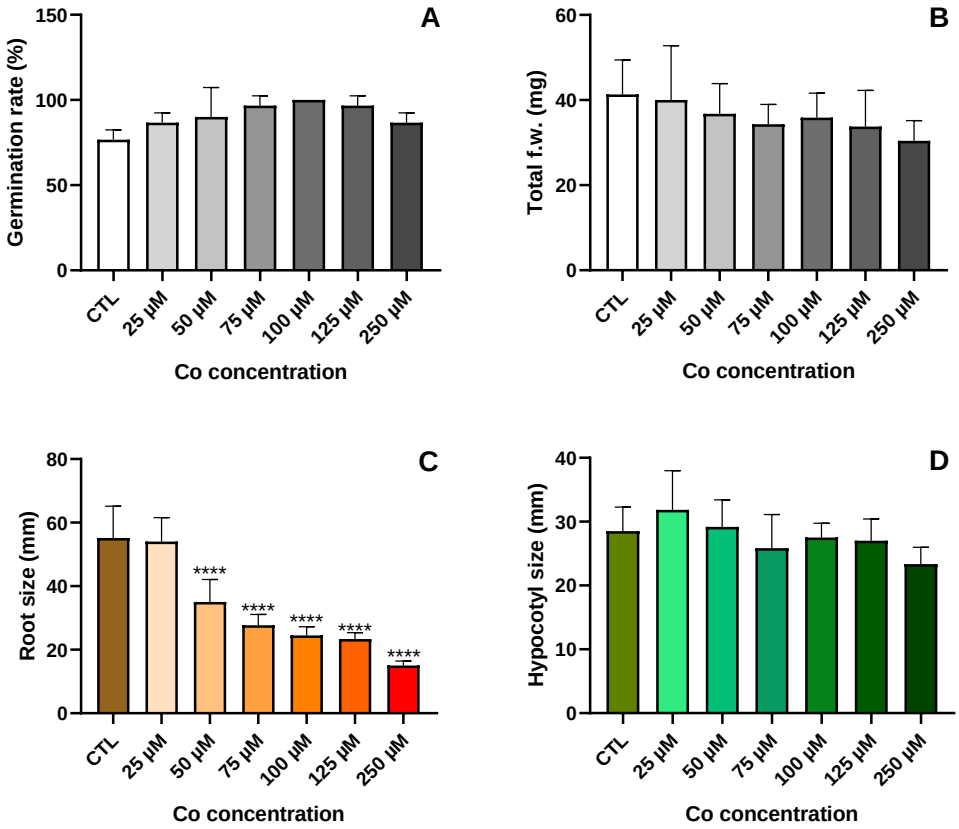

Figure 2 – Germination rate (A), total biomass (B), root (C) and hypocotyl (D) length of *S. lycopersicum* seedlings grown in nutrient medium supplemented with increasing concentrations of Co (0, 25, 50, 75, 100, 125 and 250 µM) after a 5-day exposure under *in vitro* conditions. Values presented are mean ± SD. * above bars represent significant differences (according to the Dunnett test) from the control (CTL) at * $p < 0.05$, ** $p < 0.01$, *** $p < 0.001$, **** $p < 0.0001$.

Figure 3 – General appearance of *S. lycopersicum* seedlings grown in nutrient medium supplemented with increasing concentrations of Co (0, 25, 50, 75, 100, 125 and 250 µM) after a 5-day exposure under *in vitro* conditions.

3.1.2. Effects of increasing EE2 concentrations on seed germination and early development

So as to test the effects of EE2 on tomato seeds' germination and seedling growth, a germination assay with different concentrations of this contaminant was conducted. The concentrations were as follows: 0, 100, 250, 500, 750 and 1000 $ng.L^{-1}$. Germination rate, total biomass and root length were not affected (Figure 4 A, B and C, respectively). Only the hypocotyl length parameter showed significant differences, having the EE2 1000 $ng.L^{-1}$ group increased by 11 % when compared to the CTL (Figure 4 D).

Even though EE2 had little impact in the tested parameters in a single exposure, this compound may still have an effect in tomato's seed germination and seedling growth when in a coexposure situation with Co. To test that hypothesis, the concentrations of EE2 (maintaining the same range) selected were: the lowest (100 $ng.L^{-1}$), middle (500 $ng.L^{-1}$) and highest (1000 $ng.L^{-1}$).

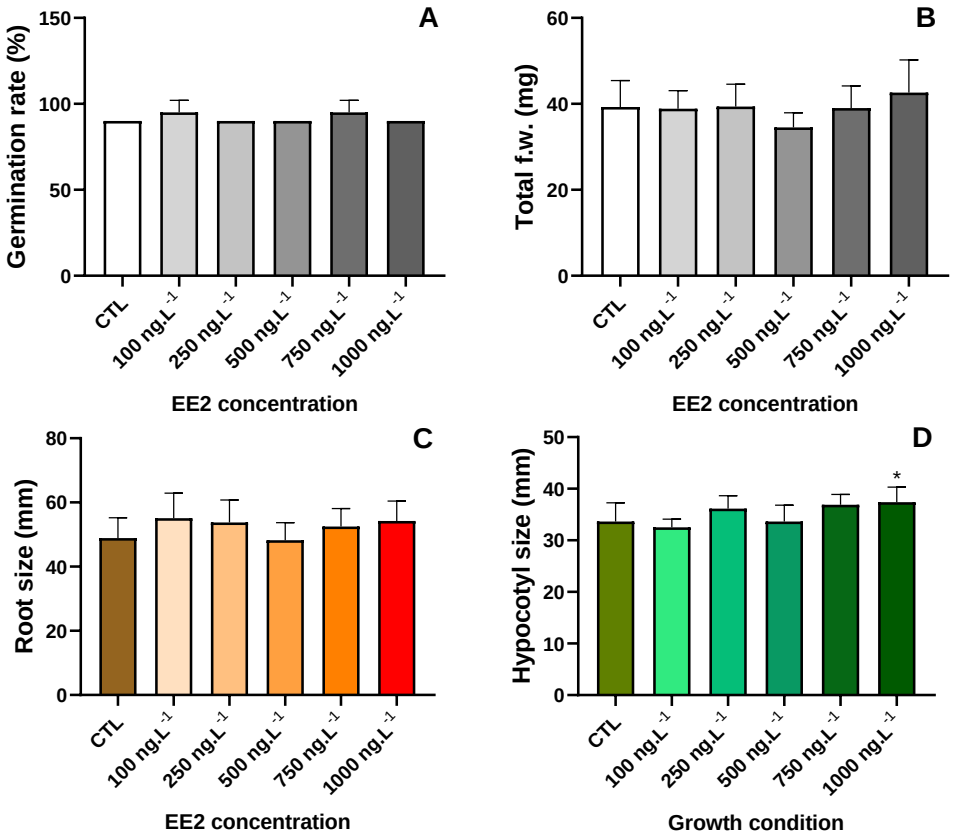

Figure 4 – Germination rate (A), total biomass (B), root (C) and hypocotyl (D) length of *S. lycopersicum* seedlings grown in nutrient medium supplemented with increasing concentrations of EE2 (0, 100, 250, 500, 750 and 1000 ng.L^{-1}) after a 5-day exposure under *in vitro* conditions. Values presented are mean ± SD. * above bars represent significant differences (according to the Dunnett test) from the CTL at * $p < 0.05$, ** $p < 0.01$, *** $p < 0.001$, **** $p < 0.0001$.

3.1.3. Effects of Co and EE2 coexposure on seed germination and early plant development

To understand how the coexposure to EE2 might influence the effects of Co on *S. lycopersicum* seed germination and seedling growth, a germination assay was performed, testing the optimized concentration of Co (50 µM) together with increasing levels of EE2 (100, 500 and 1000 ng.L^{-1}). The germination rate was not significantly affected (Figure 5 A). Total biomass decreased significantly in the Co + 100 ng.L^{-1} EE2 and Co + 1000 ng.L^{-1} EE2 groups (37 and 23 %, respectively), when compared to the CTL (Figure 5 B). Regarding root length, there was a significant decrease of 22 % in the Co group, comparing to the CTL, and of 19 % when comparing to the Co + 500 ng.L^{-1}

EE2 group (Figure 5 A). As to the hypocotyl size, there was a significant decrease in the Co, Co + 100 ng.L^{-1} EE2 and Co + 1000 ng.L^{-1} EE2 groups of 27, 49 and 21 %, comparing to the CTL (Figure 5 B).

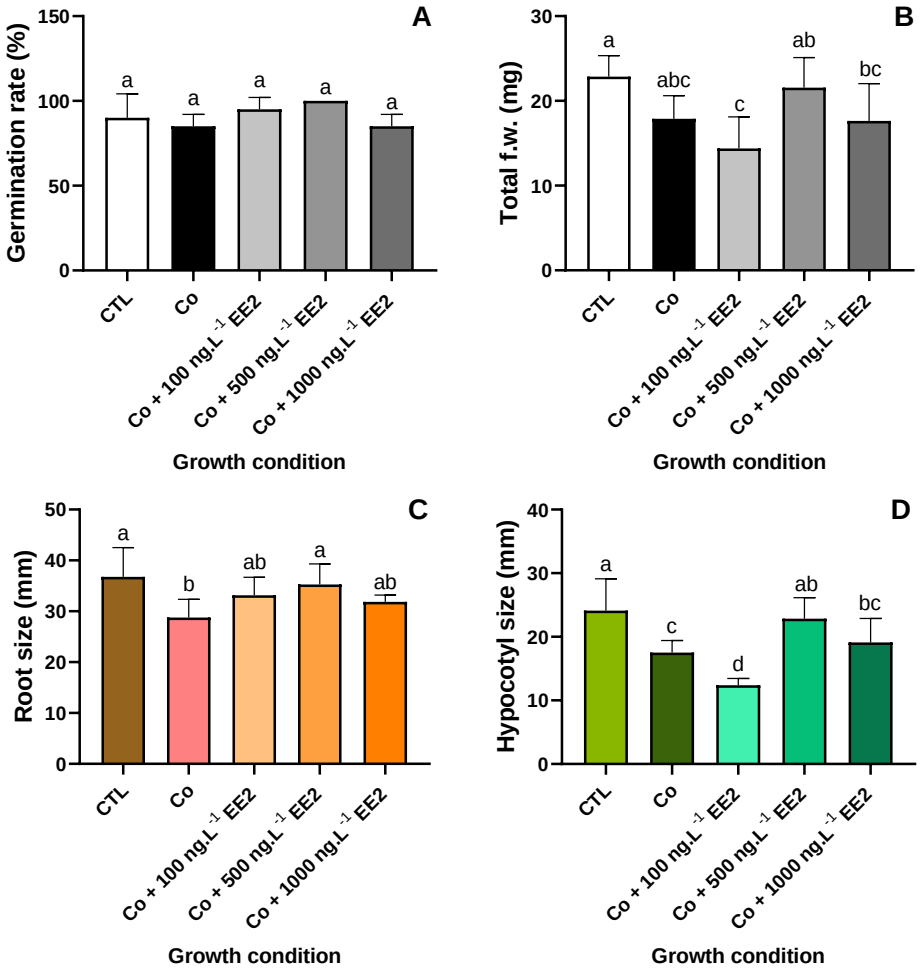

Figure 5 – Germination rate (A), total biomass (B), root (C) and hypocotyl (D) length of *S. lycopersicum* seedlings grown in plain nutrient medium (CTL), nutrient medium supplemented with 50 µM Co (Co), or with 50 µM Co and increasing concentrations of EE2 (100, 500 and 1000 ng.L^{-1}) after a 5-day exposure under in vitro conditions. Values presented are mean ± SD. Different letters above bars represent significant differences (according to the Tukey test) at $p \leq 0.05$.

Given the similarity in biometric data regarding the CTL and Co + 500 ng.L^{-1} EE2 groups, it appears that EE2, at this concentration, helped to mitigate the negative effects imposed by Co at 50 µM. Thus, this was the selected concentration of EE2 to be used in the prolonged exposure assay. At this point, both contaminants' concentrations had been

optimized: 50 µM for Co and 500 ng.L^{-1} for EE2. These would be tested in single and combined exposures.

3.1.4. Effects of a prolonged exposure to Co and EE2 on tomato plants biometry and morphology

Ensuing a 5-week growth period, the plants from the different groups (CTL, Co, EE2 and Co+EE2) were collected, visually evaluated and their biometric data analyzed. As observed in Figure 6, plants treated with EE2 had a higher shoot size when compared to the others.

Plants exposed to Co, either in single or combined exposure with EE2, showed interfascicular chlorosis in some leaves and even necrotic spots in the older leaves (Figure 7). An interesting aspect to be mentioned is the time at which these symptoms manifested, since they started to develop sooner in the coexposure group (after 2 weeks) than in the Co group (after 3 weeks). Although the chlorotic effect in the younger leaves appears to be more noticeable in the plants exposed to both contaminants, the necrotic spots seem to be more severe in the plants exposed to Co by itself.

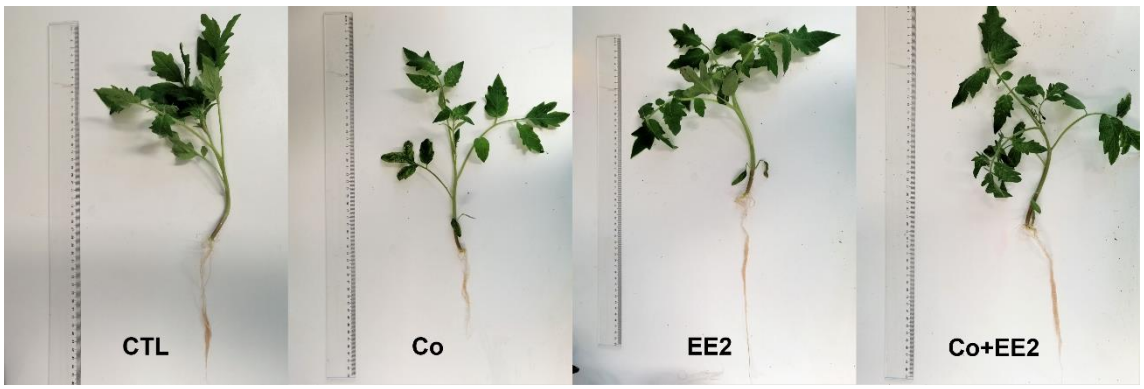

Figure 6 – Morphology of *S. lycopersicum* plants grown for 30 days in vermiculite:perlite (1:1), watered with: nutrient medium (CTL), nutrient medium supplemented with 50 µM Co (Co), nutrient medium supplemented with 500 ng.L^{-1} EE2 (EE2) or nutrient medium supplemented with both Co and EE2 (Co+EE2), in their respective concentrations. The same 50 cm ruler was used in all pictures.

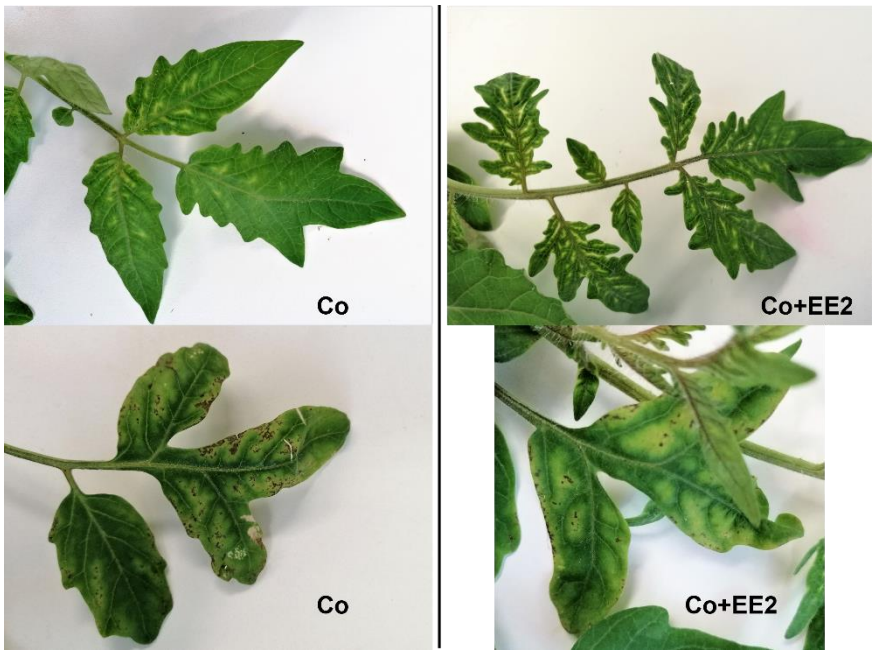

Figure 7 – Leaf morphology details of *S. lycopersicum* plants grown for 30 days in vermiculite:perlite (1:1), watered with: nutrient medium supplemented with 50 µM Co (Co) or nutrient medium supplemented with 50 µM Co and 500 ng.L^{-1} EE2 (Co+EE2). The upper images are from young leaves (3rd emergent) and the bottom ones from the oldest leaves.

Regarding the biometric data, all groups presented similar values of root length (Figure **8** A). However, concerning root biomass, Co induced a significant decrease of 46 % comparing to the CTL (Figure 8 B). In the case of shoot length, the EE2 single exposure showed a significant increase when compared to the other groups: of 28 % to CTL, 38 % to Co and 21 % to Co+EE2 (Figure 8 C). As to shoot biomass, significant differences were detected when comparing the Co group to the others, as it decreased 41 %, 43 % and 42 % regarding the CTL, EE2 and Co+EE2 groups, respectively (Figure **8** D).

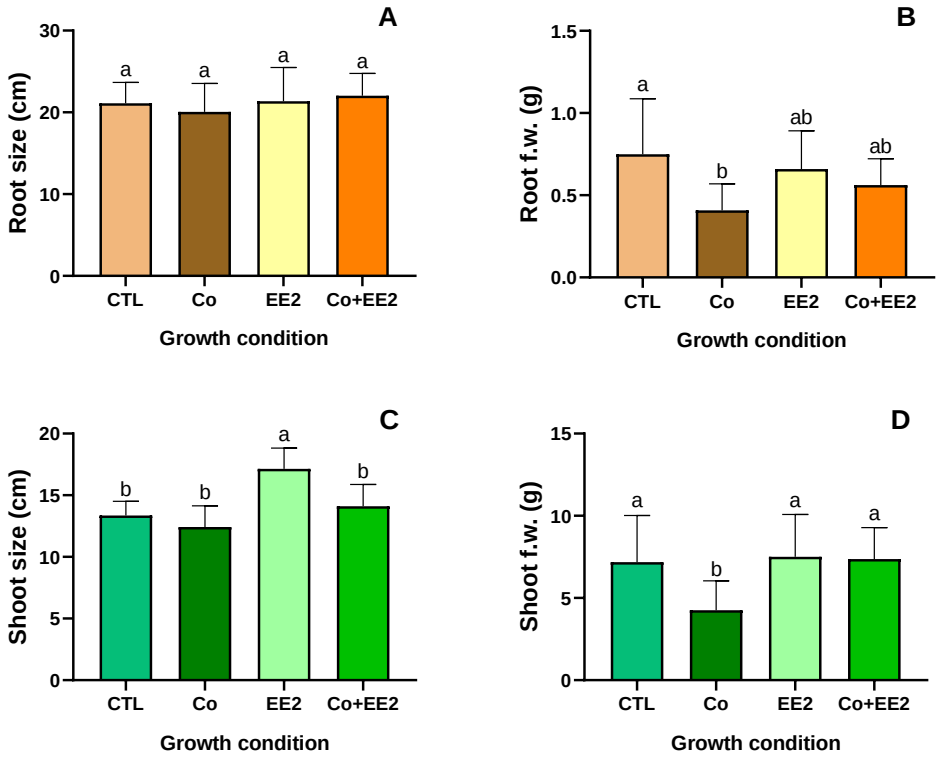

Figure 8– Root size (A) and biomass (B) and shoot size (C) and biomass (D) of *S. lycopersicum* plants grown for 30 days in vermiculite:perlite (1:1), watered with: nutrient medium (CTL), nutrient medium supplemented with 50 µM Co (Co), nutrient medium supplemented with 500 ng.L^{-1} EE2 (EE2) or nutrient medium supplemented with both Co and EE2 (Co+EE2), in their respective concentrations. Values presented are mean ± SD. Different letters above bars represent significant differences (according to the Tukey test) at $p \leq 0.05$.

3.2. Effects of Co and EE2 on leaf physiology

3.2.1. LWC

The LWC was assessed in terms of percentage of the total biomass. The EE2 group showed significantly lower levels when compared to the Co group, being reduced by 3 % (Figure 9).

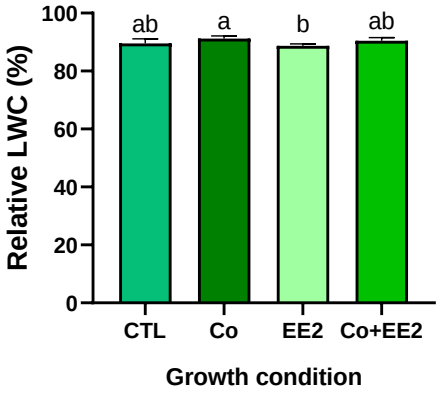

Figure 9 – Relative leaf water content of *S. lycopersicum* plants grown for 30 days in vermiculite:perlite (1:1), watered with: nutrient medium (CTL), nutrient medium supplemented with 50 µM Co (Co), nutrient medium supplemented with 500 $ng.L^{-1}$ EE2 (EE2) or nutrient medium supplemented with both Co and EE2 (Co+EE2), in their respective concentrations. Values presented are mean ± SD. Different letters above bars represent significant differences (according to the Tukey test) at $p \leq 0.05$.

3.2.2. Photosynthetic pigments

Regarding pigment concentrations, plants single exposed to EE2 showed significant increases in all measured pigments except for Lut, with Chl_a, Chl_b, Chl_{a+b} and β-car increasing by 27 %, 29 %, 26 % and 39 %, respectively, when comparing to the CTL (Figure 10).

Exposure to Co led to a significant increase in Chl_a and Chl_{a+b} by 22 % and 20 %, respectively. This was also the only treatment that caused a significant increase in Lut (26 %). The plants from the coexposure treatment displayed a significant increase in Chl_a (22 %), Chl_{a+b} (20 %) and β-car (38 %), when comparing to the CTL, and a decrease in Lut (28 %) when comparing to plants exposed to Co by itself.

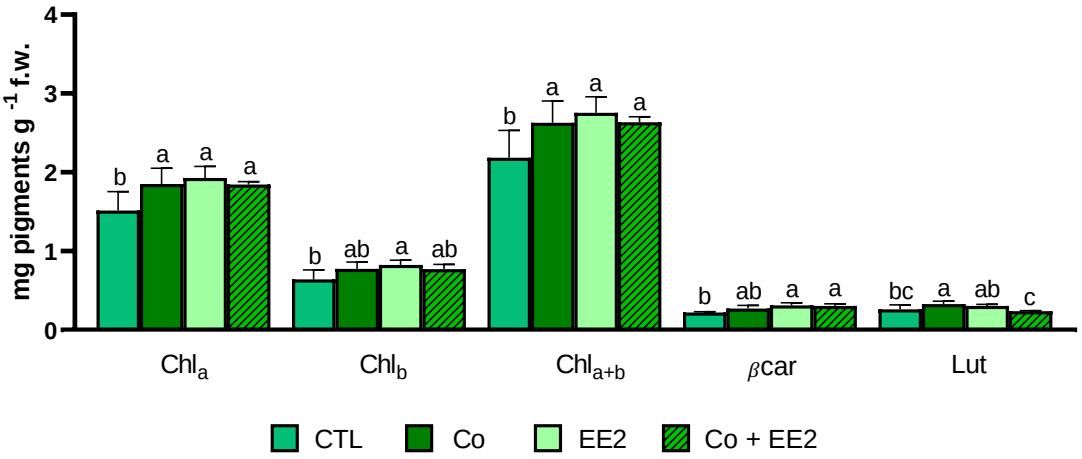

Figure 10 – Pigment concentrations expressed in mg per g of fresh weight in leaf disks of *S. lycopersicum* plants grown for 30 days in vermiculite:perlite (1:1), watered with: nutrient medium (CTL), nutrient medium supplemented with 50 µM Co (Co), nutrient medium supplemented with 500 ng.L^{-1} EE2 (EE2) or nutrient medium supplemented with both Co and EE2 (Co+EE2), in their respective concentrations. Values presented are mean ± SD. Within each pigment's concentration, different letters above bars represent significant differences (according to the Tukey test) at $p \leq 0.05$. Chl_a: Chlorophyl a; Chl_b: Chlorophyl b; Chl_{a+b}: total chlorophyl; βcar: βCarotene; Lut: lutein.

Data regarding pigment concentrations expressed in mg pigment mg^{-1} d. w. can be found in Supplemental Data 1.

3.2.3. Histochemical starch quantification

The histochemical coloration of starch grains, where the intensity of the blue color is indicative of a higher starch content, indicated that the CTL exhibited the highest starch levels, which were negatively affected by both tested contaminants, especially Co (Figure 11). Furthermore, it appears that, upon a coexposure situation, starch accumulation was partially restored back to CTL levels. As can be observed, the accumulation pattern, from higher to lower was as follows: CTL > EE2 > Co+EE2 > Co.

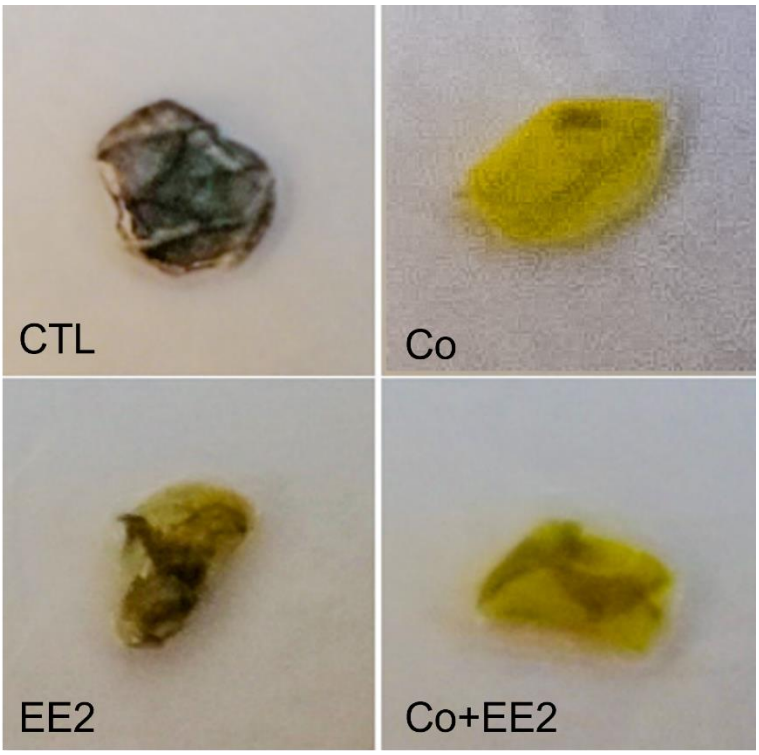

Figure 11 – Lugol staining of starch in leaf disks of *S. lycopersicum* plants grown for 30 days in vermiculite:perlite (1:1), watered with: nutrient medium (CTL), nutrient medium supplemented with 50 µM Co (Co), nutrient medium supplemented with 500 ng.L^{-1} EE2 (EE2) or nutrient medium supplemented with both Co and EE2 (Co+EE2), in their respective concentrations.

3.3. Effects of Co and EE2 on several stress biomarkers

3.3.1. Oxidative stress

In the shoots, MDA levels (indicative of LP) increased significantly (by 77 %) in the coexposure group, comparing to the CTL (Figure 12 A). In the Co and EE2 groups, there was a tendency for this parameter to increase, although not statistically significant. Regarding the roots, Co, EE2 and their combined exposure led to significantly higher levels of this parameter when compared to the CTL, increasing by 76 %, 98 % and 112 %, respectively (Figure 12 B).

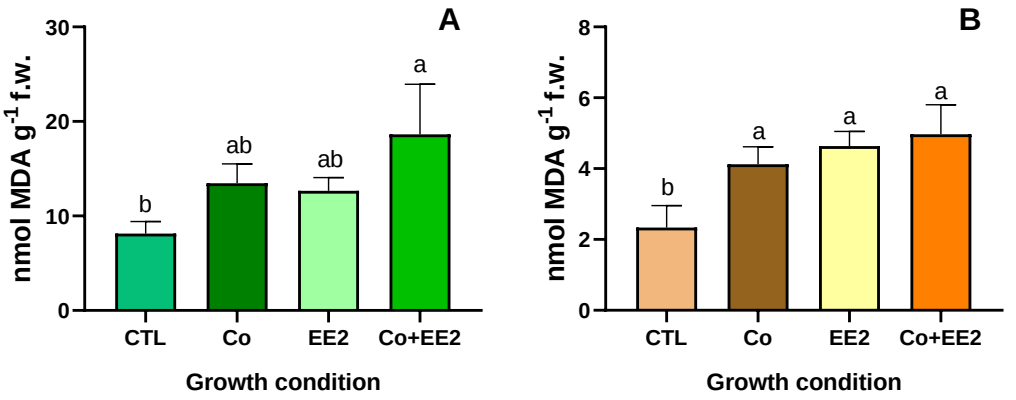

Figure 12 – MDA levels in the shoots (A) and roots (B) of *S. lycopersicum* plants grown for 30 days in vermiculite:perlite (1:1), watered with: nutrient medium (CTL), nutrient medium supplemented with 50 µM Co (Co), nutrient medium supplemented with 500 ng.L^{-1} EE2 (EE2) or nutrient medium supplemented with both Co and EE2 (Co+EE2), in their respective concentrations. Values presented are mean ± SD. Different letters above bars represent significant differences (according to the Tukey test) at $p \leq 0.05$.

Concerning H_2O_2 levels, when comparing to the CTL, plants exposed to Co, either in single or combined exposure, showed an increase of 113 % and 231 %, respectively, in the shoots (Figure 13 A) and of 189 % and 198 %, respectively, in the roots (Figure 13 B).

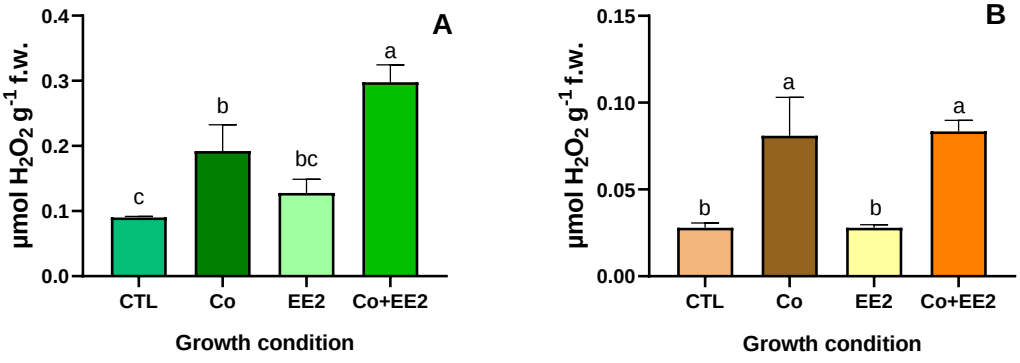

Figure 13 – H_2O_2 levels in the shoots (A) and roots (B) of *S. lycopersicum* plants grown for 30 days in vermiculite:perlite (1:1), watered with: nutrient medium (CTL), nutrient medium supplemented with 50 µM Co (Co), nutrient medium supplemented with 500 ng.L^{-1} EE2 (EE2) or nutrient medium supplemented with both Co and EE2 (Co+EE2), in their respective concentrations. Values presented are mean ± SD. Different letters above bars represent significant differences (according to the Tukey test) at $p \leq 0.05$.

3.3.2. Non-enzymatic components of the AOX system

There were no statistical differences in Pro content in the shoots (Figure 14 A). However, in the roots, Pro levels were significantly lower in the coexposure treatment, decreasing by 70 % comparing to the CTL (Figure 14 B). In both Co and EE2 treatments by themselves this parameter showed a tendency to decrease.

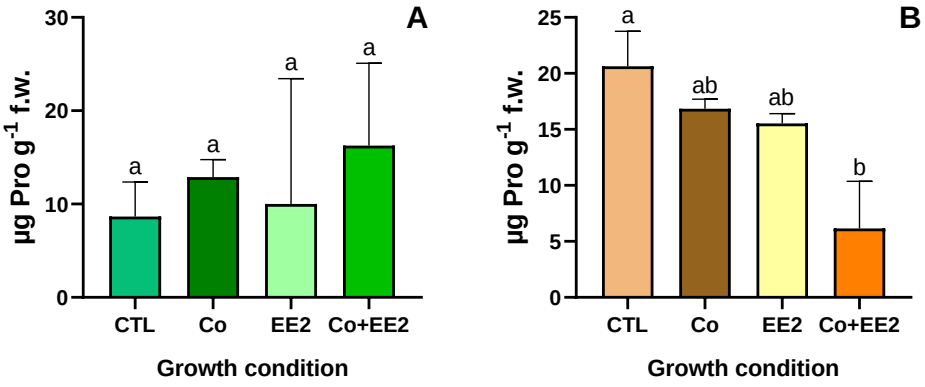

Figure 14 – Pro levels in the shoots (A) and roots (B) of *S. lycopersicum* plants grown for 30 days in vermiculite:perlite (1:1), watered with: nutrient medium (CTL), nutrient medium supplemented with 50 µM Co (Co), nutrient medium supplemented with 500 ng.L^{-1} EE2 (EE2) or nutrient medium supplemented with both Co and EE2 (Co+EE2), in their respective concentrations. Values presented are mean ± SD. Different letters above bars represent significant differences (according to the Tukey test) at $p \leq 0.05$.

As is shown in Figure 15 (A and B), GSH levels were significantly impacted: positively in shoots by the coexposure, increasing by 143 %, and negatively in roots by the exposure to EE2, decreasing by 90 %.

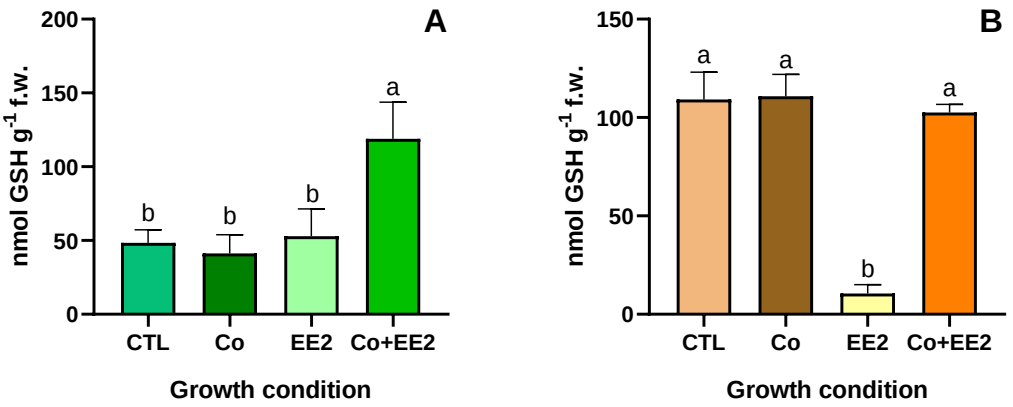

Figure 15 – GSH levels in the shoots (A) and roots (B) of *S. lycopersicum* plants grown for 30 days in vermiculite:perlite (1:1), watered with: nutrient medium (CTL), nutrient medium supplemented with 50 µM Co (Co), nutrient medium supplemented with 500 ng.L^{-1} EE2 (EE2) or nutrient medium supplemented with both Co and EE2 (Co+EE2), in their respective concentrations. Values presented are mean ± SD. Different letters above bars represent significant differences (according to the Tukey test) at $p \leq 0.05$.

Results regarding total, reduced (AsA) and oxidized (DHA) ascorbate levels, as well as their ratios, are presented in Figure 16 and Figure 17. These results are also compiled in a table (see Supplemental Data 2).

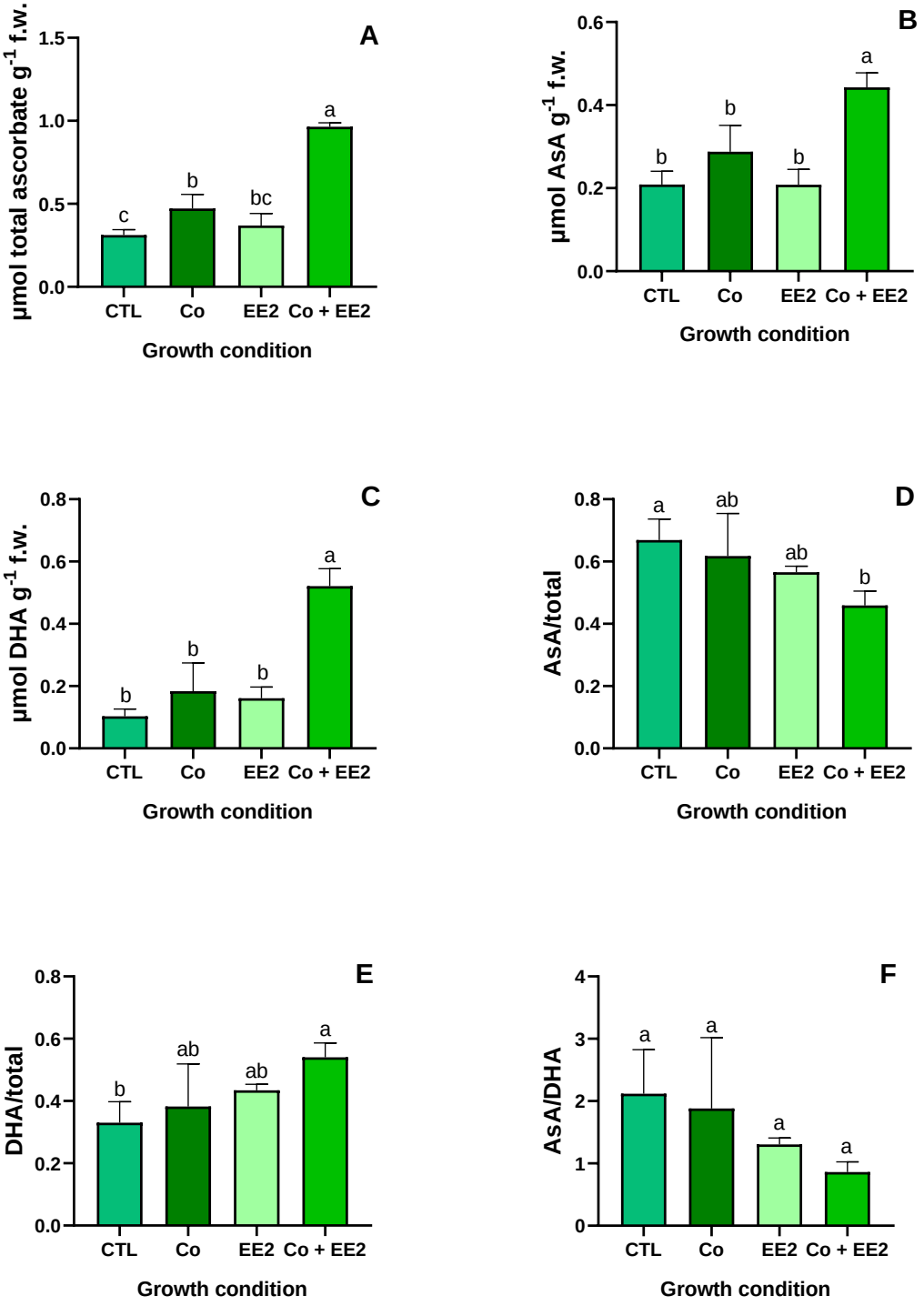

Figure 16 – Total (A), reduced (B) and oxidized (C) ascorbate levels and ratios (D, E and F) in the shoots of *S. lycopersicum* plants grown for 30 days in vermiculite:perlite (1:1), watered with: nutrient medium (CTL), nutrient medium supplemented with 50 µM Co (Co), nutrient medium supplemented with 500 ng.L^{-1} EE2 (EE2) or nutrient medium supplemented with both Co and EE2 (Co+EE2), in their respective concentrations. Values presented are mean ± SD. Different letters above bars represent significant differences (according to the Tukey test) at $p \leq 0.05$.

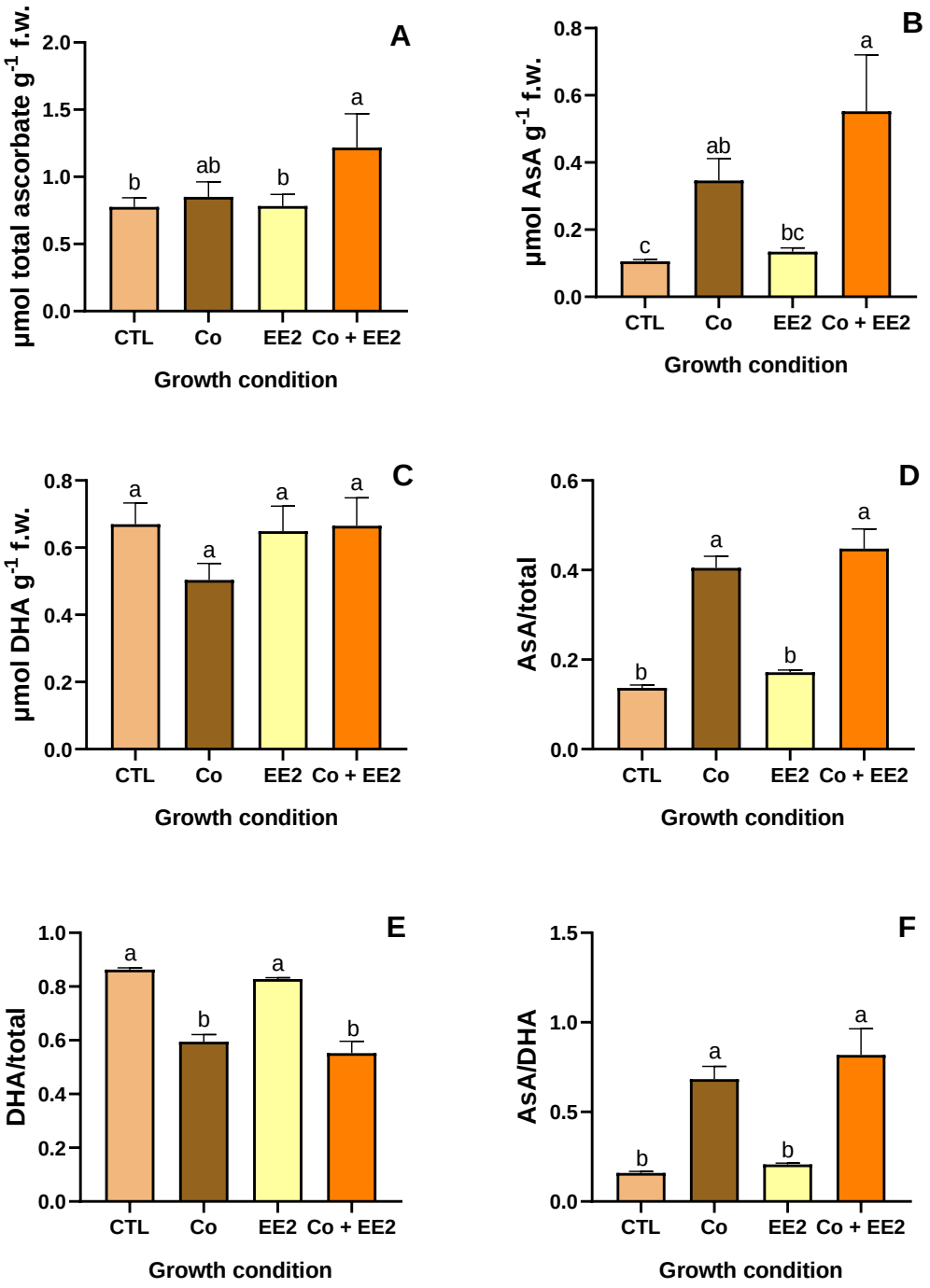

Figure 17 – Total (A), reduced (B) and oxidized (C) ascorbate levels and ratios (D, E and F) in the roots of *S. lycopersicum* plants grown for 30 days in vermiculite:perlite (1:1), watered with: nutrient medium (CTL), nutrient medium supplemented with 50 µM Co (Co), nutrient medium supplemented with 500 ng.L^{-1} EE2 (EE2) or nutrient medium supplemented with both Co and EE2 (Co+EE2), in their respective concentrations. Values presented are mean ± SD. Different letters above bars represent significant differences (according to the Tukey test) at $p \leq 0.05$.

In the aerial part of the plant, when comparing to the CTL, exposure to Co by itself presented a significant increase (by 51 %) in total ascorbate levels. In the Co+EE2 treated plants, the Asa, DHA and total ascorbate concentrations were significantly higher, not only in comparison to CTL (112 %, 406 % and 209 %, respectively) but also to Co (54 %, 184 % and 105 %, respectively). When comparing to the CTL, the coexposure to Co and EE2 also produced a significant decrease in AsA/total ascorbate (by 31 %) and increase DHA/total ascorbate (by 64 %), but not in AsA/DHA, although there was a tendency to decrease this ratio in this treatment.

In the roots, plants exposed to Co by itself showed a significant increase, when compared to the CTL, in AsA levels (by 226 %) and in the AsA/total ascorbate and AsA/DHA ratios (by 196 % and 329 %, respectively), and a decrease in the DHA/total ascorbate ratio (by 31 %). In the coexposure group, results were very similar to the single exposure to Co, as there was a significant increase in AsA levels (by 421 %) and in the AsA/total and AsA/DHA ratios (by 228 % and 414 %, respectively), and a decrease in the DHA/total ratio (by 36 %), comparing to the CTL. However, the increase in AsA levels was more pronounced and the DHA levels were similar to the CTL, resulting in a significant increase in total ascorbate levels (by 84 %), also when comparing to the CTL.

In both shoots and roots, the response from the plants exposed to EE2 was very similar to the CTL, with no statistical differences being detected between these groups.

3.3.3. Total soluble protein content

Although there were no statistical differences in the shoots between all treatments (Figure 18 A), in the roots, the coexposure showed a significant increase (up to 42 %) in this parameter, when comparing to all other experimental groups (Figure 18 B).

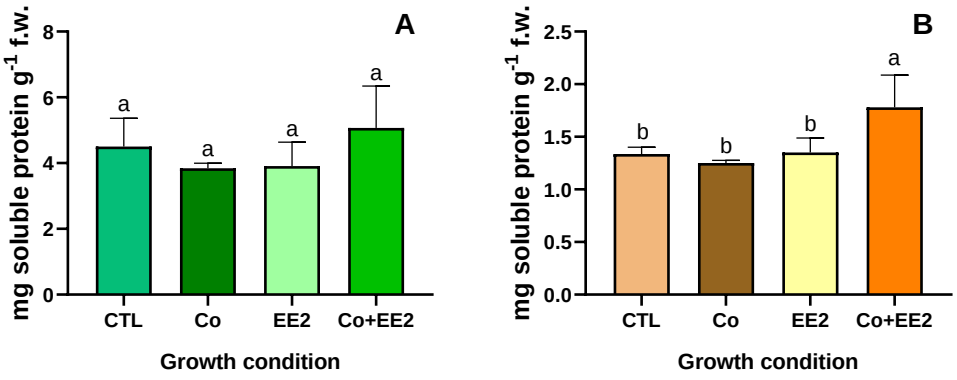

Figure 18 – Total soluble protein levels in the shoots (A) and roots (B) of *S. lycopersicum* plants grown for 30 days in vermiculite:perlite (1:1), watered with: nutrient medium (CTL), nutrient medium supplemented with 50 µM Co (Co), nutrient medium supplemented with 500 ng.L^{-1} EE2 (EE2) or nutrient medium supplemented with both Co and EE2 (Co+EE2), in their respective concentrations. Values presented are mean ± SD. Different letters above bars represent significant differences (according to the Tukey test) at $p \leq 0.05$.

3.3.4. Enzymatic component of the AOX system

To understand how the plants' enzymatic component of the antioxidant system was responding to the exposure to Co and EE2, either alone and combined, the activities of some key AOX enzymes (SOD, APX, CAT, DHAR and GR) were measured.

The activity of SOD in the shoots decreased significantly with Co (by 28 %), when comparing to CTL (Figure 19 A). In the roots, no statistical relevance was achieved, although a tendency for a reduced SOD activity could be perceived upon single exposure to the metal (Figure 19 B).

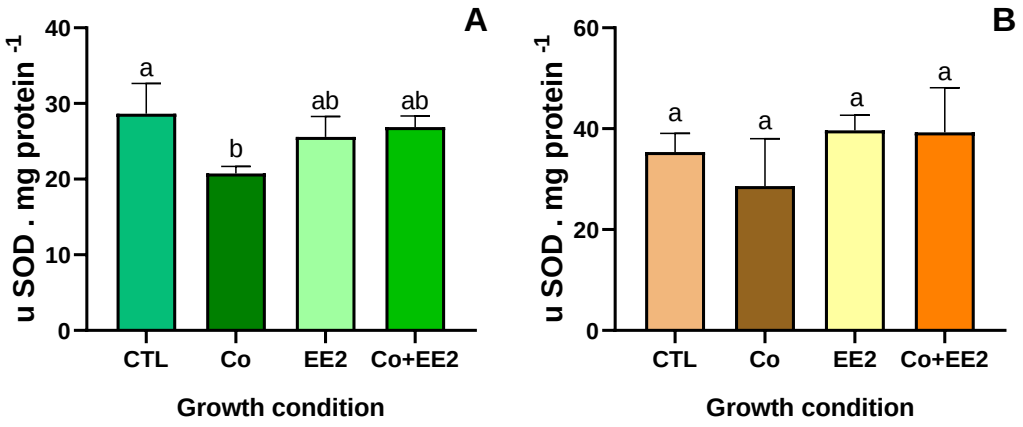

Figure 19 – SOD activity levels in the shoots (A) and roots (B) of *S. lycopersicum* plants grown for 30 days in vermiculite:perlite (1:1), watered with: nutrient medium (CTL), nutrient medium supplemented with 50 µM Co (Co), nutrient medium supplemented with 500 ng.L^{-1} EE2 (EE2) or nutrient medium supplemented with both Co and EE2 (Co+EE2), in their respective concentrations. Values presented are mean ± SD. Different letters above bars represent significant differences (according to the Tukey test) at $p \leq 0.05$.

CAT activity showed no statistically significant differences between groups, in both shoots and roots (Figure 20 A and B). There was, however, a tendency to decrease in the EE2 group in the shoots, and to increase in the roots for the plants exposed to EE2, both by itself and in the combined exposure.

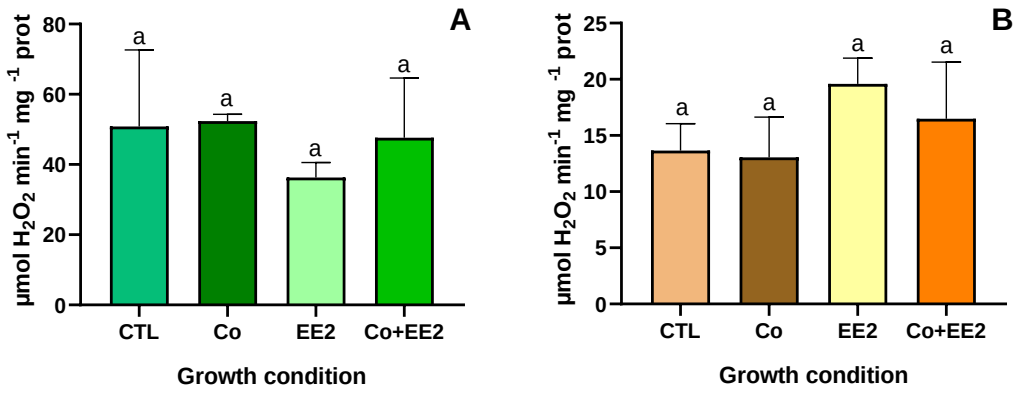

Figure 20 – CAT activity levels in the shoots (A) and roots (B) of *S. lycopersicum* plants grown for 30 days in vermiculite:perlite (1:1), watered with: nutrient medium (CTL), nutrient medium supplemented with 50 µM Co (Co), nutrient medium supplemented with 500 ng.L^{-1} EE2 (EE2) or nutrient medium supplemented with both Co and EE2 (Co+EE2), in their respective concentrations. Values presented are mean ± SD. Different letters above bars represent significant differences (according to the Tukey test) at $p \leq 0.05$.

Regarding APX activity in the shoots, the groups treated with EE2, either alone or in coexposure with Co, presented a significant reduction when compared to either the CTL (around 60 %) or Co (around 70 %) (Figure 21 A). In the roots, there were no significant differences, however, the same pattern of the shoots could also be noticed (Figure 21 B).

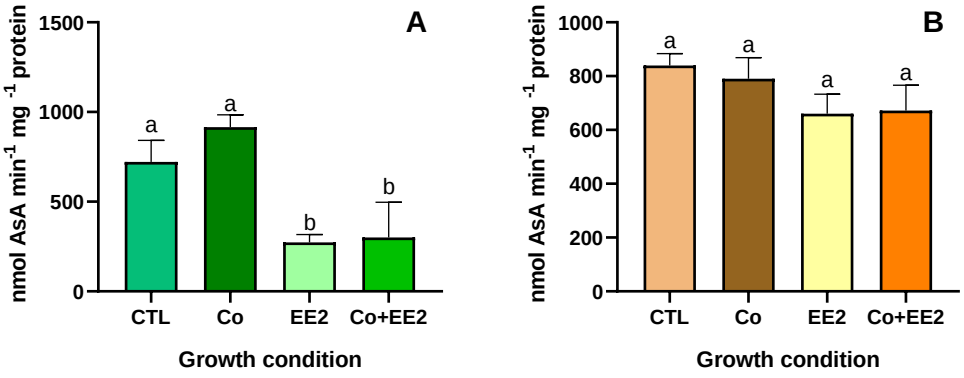

Figure 21 – APX activity levels in the shoots (A) and roots (B) of *S. lycopersicum* plants grown for 30 days in vermiculite:perlite (1:1), watered with: nutrient medium (CTL), nutrient medium supplemented with 50 µM Co (Co), nutrient medium supplemented with 500 ng.L^{-1} EE2 (EE2) or nutrient medium supplemented with both Co and EE2 (Co+EE2), in their respective concentrations. Values presented are mean ± SD. Different letters above bars represent significant differences (according to the Tukey test) at $p \leq 0.05$.

DHAR activity showed no statistically significant differences between groups, in both shoots and roots (Figure 22 A and B).

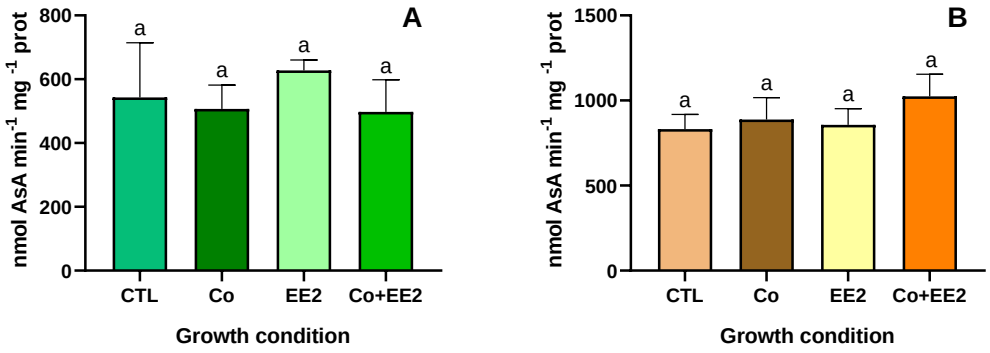

Figure 22 – DHAR activity levels in the shoots (A) and roots (B) of *S. lycopersicum* plants grown for 30 days in vermiculite:perlite (1:1), watered with: nutrient medium (CTL), nutrient medium supplemented with 50 µM Co (Co), nutrient medium supplemented with 500 ng.L^{-1} EE2 (EE2) or nutrient medium supplemented with both Co and EE2 (Co+EE2), in their respective concentrations. Values presented are mean ± SD. Different letters above bars represent significant differences (according to the Tukey test) at $p \leq 0.05$.

In the aerial part of the plants, GR activity was reduced upon exposure to EE2, either alone (63 %) or in combination with Co (47 %), when compared to the CTL (Figure 23 A). In response to Co, no major changes were observed, although a tendency for plants to increase GR activity could be perceived. In the roots, significant differences were only detected in plants exposed to both Co and EE2, with an increase of 61 % comparing to the CTL (Figure 23 B).

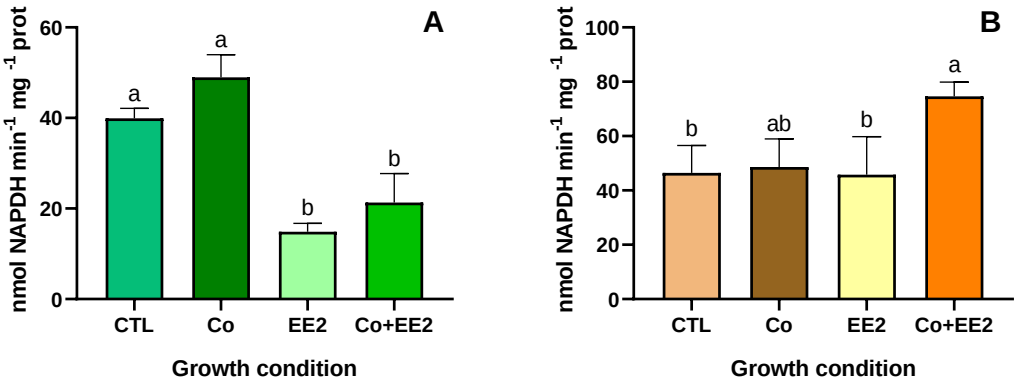

Figure 23 – GR activity levels in the shoots (A) and roots (B) of *S. lycopersicum* plants grown for 30 days in vermiculite:perlite (1:1), watered with: nutrient medium (CTL), nutrient medium supplemented with 50 µM Co (Co), nutrient medium supplemented with 500 $ng.L^{-1}$ EE2 (EE2) or nutrient medium supplemented with both Co and EE2 (Co+EE2), in their respective concentrations. Values presented are mean ± SD. Different letters above bars represent significant differences (according to the Tukey test) at $p \leq 0.05$.

3.3.1. GST activity

In the shoots, GST activity was stimulated by EE2, either in single or coexposure, by 80 % and 105 %, respectively, in relation to the CTL (Figure 24 A). In the Co group there was a slight tendency to increase in this parameter, comparing to the CTL. In roots, no changes were found among groups (Figure 24 B).

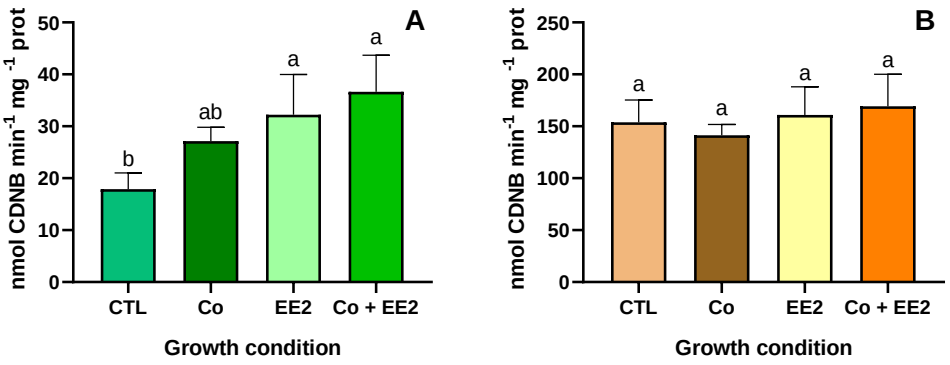

Figure 24 – GST activity levels in the shoots (A) and roots (B) of *S. lycopersicum* plants grown for 30 days in vermiculite:perlite (1:1), watered with: nutrient medium (CTL), nutrient medium supplemented with 50 µM Co (Co), nutrient medium supplemented with 500 ng.L^{-1} EE2 (EE2) or nutrient medium supplemented with both Co and EE2 (Co+EE2), in their respective concentrations. Values presented are mean ± SD. Different letters above bars represent significant differences (according to the Tukey test) at $p \leq 0.05$.

3.4. Effects of Co and EE2 on transcript accumulation patterns

Semi-quantitative quantification of gene expression

After quantification and quality assessment of the extracted RNA, which was shown to be stable and of good quality, as the rRNA bands were well defined and no smear was detected (Figure 25), a semi-quantitative RT-PCR analysis permitted a general understanding of how Co and EE2, by themselves or in a combined exposure, interfered with transcript accumulation of some genes related to key macromolecules and enzymes involved in plant detoxification pathways.

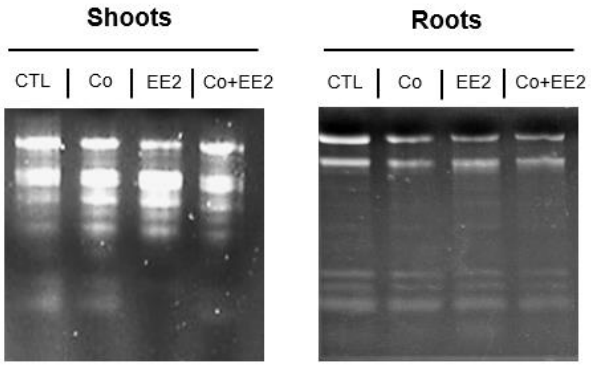

Figure 25 – Typical 1 % (w/v) agarose gel analysis of 300 ng the total RNA extracted from *S. lycopersicum* plants grown for 30 days in vermiculite:perlite (1:1), watered with: nutrient medium (CTL), nutrient medium supplemented with 50 µM Co (Co), nutrient medium supplemented with 500 ng.L^{-1} EE2 (EE2) or nutrient medium supplemented with both Co and EE2 (Co+EE2), in their respective concentrations.

3.4.1. Effects of Co and EE2 on metallothioneins-encoding genes' expression

In the roots, *MT1* mRNA accumulation increased the most in the plants exposed to Co by itself, with a slight increase in the EE2 and coexposure groups (Figure 26). As to *MT2*'s transcripts in the same organ, there was a higher accumulation for the Co treatment and a lower one for EE2. Finally, *MT4* showed higher levels of transcription in both contaminants' single exposure groups.

In the aerial part of the plants, *MT1* presented higher levels of transcript accumulation in the plants single exposed to EE2, but there were no detected transcripts in the coexposure situation. For *MT2*, gene expression was reduced in both contaminants' single exposure groups. *MT4* suffered a loss of transcripts accumulation in the coexposure treatment. *MT3* showed no detectable transcript accumulation for either organ in any group (data not shown).

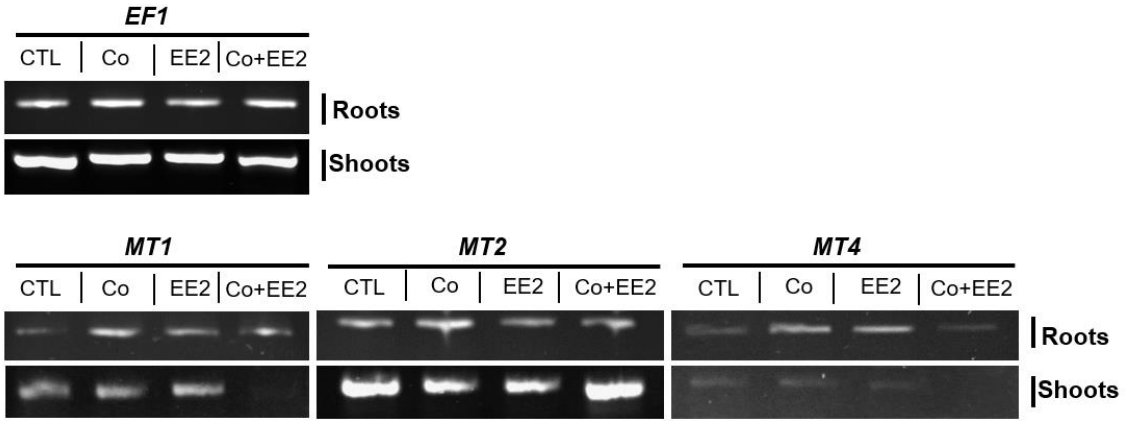

Figure 26 – Typical results for *MT1*, *MT2*, and *MT4* semi-quantitative RT-PCR analysis by 1 % (w/v) agarose gel electrophoresis in *S. lycopersicum* plants grown for 30 days in vermiculite:perlite (1:1), watered with: nutrient medium (CTL), nutrient medium supplemented with 50 µM Co (Co), nutrient medium supplemented with 500 $ng.L^{-1}$ EE2 (EE2) or nutrient medium supplemented with both Co and EE2 (Co+EE2), in their respective concentrations.

3.4.2. Effects of Co and EE2 on glutathione metabolism-related enzymes' gene expression

In the roots, plastidic GR (GR_{plast}) mRNA accumulation increased in all treatments (Figure 27). As to *GSTU*'s transcripts in the same organ, there was a lower accumulation in the coexposure group. For *PCS* and *γ-ECS*, expression was the lowest in the coexposure group, with a slight decrease in the EE2 group.

In the shoots, GR_{plast} mRNA suffered an increase in the Co group, and a noticeable decrease in the coexposure. *GSTU*'s transcript accumulation was the highest in the EE2 group, followed by the Co group, and was the lowest in the coexposure group. Both *PCS* and *γ-ECS* showed higher levels of transcription in the Co group, but no detectable levels in the coexposure group.

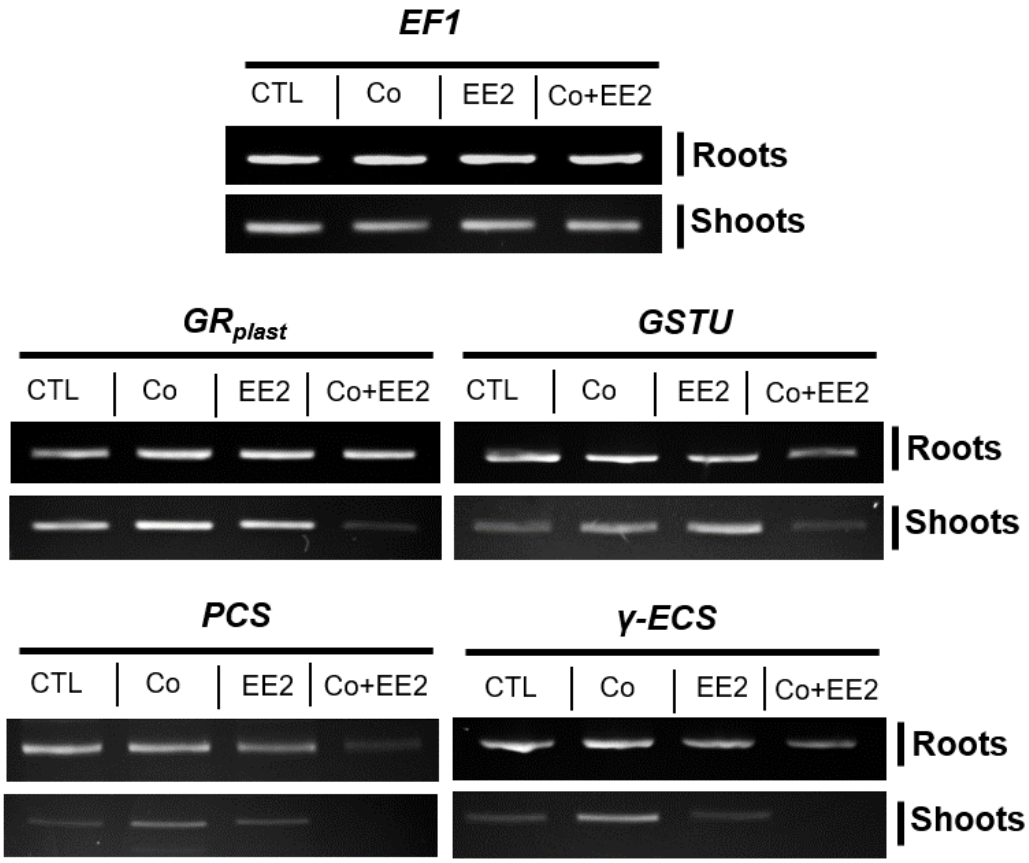

Figure 27 – Typical results for GR_{plast}, *GSTU*, *PCS* and *γ-ECS* semi-quantitative RT-PCR analysis by 1 % (w/v) agarose gel electrophoresis in *S. lycopersicum* plants grown for 30 days in vermiculite:perlite (1:1), watered with: nutrient medium (CTL), nutrient medium supplemented with 50 μM Co (Co), nutrient medium supplemented with 500 $ng.L^{-1}$ EE2 (EE2) or nutrient medium supplemented with both Co and EE2 (Co+EE2), in their respective concentrations.

4. Discussion

4.1. Co and EE2's influence on germination and seedling growth

To assess the impact of Co and EE2 on tomato seed germination and seedling growth, tomato seeds were germinated under exposure to these pollutants and, after five days of growth (after inoculation), their effects were examined. The results evidenced that neither contaminant (alone or in a coexposure scenario) had a significant effect on seed germination. This falls in line with previous reports with different types of pollutants (namely other HMs and PPCPs) where germination was only inhibited after very high and toxic dosages (Lopez-Luna et al., 2009; Chaoui and El Ferjani, 2013; Pan and Chu, 2016; Bartrons and Peñuelas, 2017). This phenomenon can be explained by the protection conferred to the seed by the seed coat (Li et al., 2005; Akinci and Akinci, 2010) protecting internal tissues from contaminant entrance.

Regarding the germination assay where the seeds were only exposed to Co, there was an evident dose-dependent reduction in the root length, starting at the 50 μM concentration. As reported by Jayakumar et al. (2008), Co may have inhibited root growth directly by suppressing cell division and elongation, limiting the uptake and translocation of nutrients and, thus, inducing mineral deficiency. The other biometric parameters (hypocotyl length and total biomass) were not affected. This pattern has been documented in several other studies, with the root being the most sensitive portion of the plant, while the aerial part's growth is much less likely to be significantly inhibited (An et al., 2009; Pan and Chu, 2016). The fact that only root length was affected can be explained by the indirect effects of the short duration of the trial. Since the roots represent the contact point between the plants and the medium, it makes sense that this organ manifested symptoms of the respective toxicity earlier. The lack of effect in the hypocotyl may be due to the discharge of nutrients from the cotyledons or endosperm countering the HMs' toxic effect (Chen et al., 2011).

The seedlings grown in a single exposure to EE2 showed an increased hypocotyl length only with the highest tested concentration (1000 $ng.L^{-1}$), whereas root size and total biomass were not affected. There is currently no data regarding the effect of EE2 on seedling growth, however, Karnjanapiboonwong et al. (2011) reported that, in *Phaseolus vulgaris* L. seedlings grown in sand watered with EE2 (1$\mu g.g^{-1}$ sand), EE2 uptake only

started after 7 days. Assuming a similar uptake rate, then it would explain the lack of effects for the lower concentrations. Similarly, Chaoui and El Ferjani (2013) described no significant changes in embryo elongation of *Lens culinaris* exposed to β-estradiol (1 μM). The detected effect for the higher concentration could be attributed to a greater uptake due to more molecules being present. In fact, a linear relationship has been discovered between the root concentration and the application dose of emerging organic contaminants (Hurtado et al., 2016).

When exposed to Co and EE2 simultaneously, tomato seedlings presented higher biometric values (root and hypocotyl length and total biomass) in the Co + 500 $ng.L^{-1}$ EE2 situation than in the Co treatment, with values similar to the CTL. These results indicate that this concentration of EE2 reversed the inhibitory effects of Co on seedling growth. Similar results were obtained by Chaoui and El Ferjani (2013), where β-estradiol protected *Lens culinaris* from embryo growth reduction induced by either Cd or Cu, when the seeds were simultaneously exposed to the estrogen and the HM.

Regarding the other tested concentrations, however, the pattern was different. At the highest concentration (1000 $ng.L^{-1}$), the values were not significantly higher than the ones obtained in the Co situation, although the same tendency than the Co + 500 $ng.L^{-1}$ EE2 situation was found. This may be due to an excess supply of this hormone beyond the optimum concentration for the beneficial effects of EE2 regarding Co-induced stress to be detected, as it might start acting as a stressor itself (Erdal and Dumlupinar, 2011). At the lowest concentration (100 $ng.L^{-1}$), the same response was present for root length. Nevertheless, for hypocotyl length and total biomass the obtained values were significantly lower for the former and showed a tendency to decrease in the latter than in the Co situation. This is an unexpected result since steroidal hormones usually present an "inverted parabola" response curve, where low doses cause a greater response than high doses (Bircher, 2011). It might be that, at this concentration, EE2 is interacting with the seedling's hormonal system and, together with Co, is inhibiting hypocotyl growth, though there are no studies to support this theory so far.

4.2. Co and EE2's influence on plant development and growth and leaf physiology

A similar approach was performed with grown plants, where untreated seedlings were exposed to each contaminant, either in an individual or a combined exposure, for five

weeks. Since the aim of this assay was to understand if EE2 may act in a beneficial way, antagonizing the phytotoxic effects of Co, the concentration of this hormone that presented the best results regarding this hypothesis (500 $ng.L^{-1}$) was selected. The Co concentration used was that of 50 µM as it showed consistently significant differences in the germination assays.

Plants from the Co situation presented lower values of both root and shoot biomass, while root and shoot length remained similar to the CTL. These results are supported by the ones obtained by Gopal et al. (2003) who reported a decrease in tomato plants' biomass when exposed to 0.05 mM Co.

The data obtained from the plants exposed to EE2 alone showed that the only different parameter was that of shoot size, which was significantly higher than the CTL. This increase aligns with previous reports, where estrogens enhanced plant growth (Erdal and Dumlupinar, 2011; Adeel et al., 2018), although root growth was also superior in these studies. A possible explanation for this increase is that EE2 was translocated to the shoots, where it induced cell division (Janeczko and Skoczowski, 2005). In fact, the translocation of this hormone to the aerial part of the plant has already been documented by Christou et al. (2016).

Finally, plants from the coexposure group showed similar biometric levels (root and shoot size and biomass) to the CTL, indicating that EE2 antagonized the Co phytotoxic effects on these parameters. Given the proximity of this hormone to brassinosteroids, which are known to mitigate abiotic and biotic stresses when applied exogenously (Bajguz and Hayat, 2009), it is possible that EE2 might be acting in a similar way.

Overall, the results from the photosynthetic pigments' analysis appear to indicate that all treatments increased the content of these molecules in the leaves, with the exception of Lut, of which only Co induced higher levels. These results are contrary to previous reports, where an exposure to Co led to a reduction of Chls content (Ali et al., 2010; Sree et al., 2015), but align with the data in Begović et al. (2016), where Chls and Car content was stimulated by low concentrations of Co (10 µM) in *Lemna minor* L.. As to EE2, an enhancement of photosynthetic pigments induced by this hormone has been reported (Adeel et al., 2018). It is important to clarify, however, that the 1 cm disks used in this analysis were collected from the terminal portion of the foliole, where the tissue was most homogeneous (to avoid interference from vascular tissues). As a setback, the area most

affected by the interfascicular chlorosis induced by Co (most present around the vascular tissues near the base of the foliole) was not included in those disks. A reevaluation of this parameter is therefore advised (following a different protocol), as the obtained results may not be representative of the whole leaf.

Nevertheless, the macroscopic analysis showed clear interfascicular chlorosis in the younger leaves of both the Co and coexposure groups, which was more intense and appeared sooner (one week earlier) in the latter. This chlorosis may be caused by a Co-induced Fe deficiency, as described by Chatterjee and Chatterjee (2003). Furthermore, there were necrotic spots in the older leaves of both these groups, but more severe in the Co treatment. These symptoms were also present in the tomato plants treated with Co (0.2 mM) by Gopal et al. (2003). It seems EE2 aggravated the nutrient deficiency provoked by Co, possibly by inducing a process of cell division, depleting the resources faster. On the contrary, the lessening of necrosis points to a protective role of this hormone, through mechanisms of action still unknown. Moreover, the depicted depigmentation most likely had an impact on the photosynthetic rate, reducing it, which would lead to a lower production of photoassimilates, resulting in lower starch accumulation levels. This phenomenon explains the results obtained in the histochemical starch coloration, that showed that starch storage was most negatively affected in the Co and coexposure groups, being most severe in the individual exposure to Co. In fact, a decrease in starch accumulation induced by Co had previously been detected by Gopal et al. (2003), which also reported an interfascicular chlorosis and necrotic spots in the leaves, induced by Co.

Overall, these results show that EE2 had mixed effects in the leaf, leading to a quicker development of Co toxicity symptoms (in the coexposure group), demonstrated by the earlier development of chlorosis, while simultaneously protecting the older leaves from necrotic damage and slightly reducing the negative impact of Co on starch accumulation. An opposite phenomenon was reported by Chaoui and El Ferjani (2013), where 15-day-old cotyledons of lentil (*Lens culinaris* Medik.) treated with both β-estradiol and Cd or Cu showed lower levels of starch accumulation than the individual exposures to each HM, but similar to the CTL. However, the cotyledons were playing the role of source of nutrients for the seedlings' growth. Therefore, in this case, the lower levels of starch are an indicator of good seedling health, as this form of storage was being broken down to

aid plant development and growth. In the end, the protective effect of β-estradiol is still comparable to the one obtained here with EE2, although to a lesser scale in the latter.

In total, EE2 seemed to protect the plants in the coexposure treatment from some Co-induced phytotoxic effects on growth and development, as seen in the recovery of biometric values similar to the CTL, starch accumulation reduction attenuation and leaves' necrotic symptoms mitigation.

4.3. Co and EE2's effects on oxidative stress

Since previous reports have shown that both Co and EE2 can induce high ROS levels, accompanied by rises in LP degree (Karuppanapandian and Kim, 2013; Christou et al., 2016; Lwalaba et al., 2017; Adeel et al., 2018), these parameters were assessed to understand if the same pattern could also be detected in tomato plants, and how the coexposure of both contaminants might change such outcome. For this, H_2O_2 and MDA levels were evaluated in tomato plants exposed to Co and EE2, in single and combined exposures. The results showed that, in the shoots, there was an accentuated increase in H_2O_2 levels in response to Co, with an even higher level for the coexposure treatment, while EE2 by itself did not cause an increase in this parameter. The higher H_2O_2 levels in the plants exposed to Co (both alone or in the coexposure) may be explained by a disturbance in the electron transport chains (Begović et al., 2016). As to MDA levels, still in the shoots, only the coexposure led to significantly higher levels, with both contaminants' single exposure treatments leading to only slight and non-significant increases. These results imply that Co is the bigger stressor, while EE2 is acting synergistically towards a higher oxidative stress level, possibly by inducing higher levels of other ROS, such as ·OH (Foyer and Noctor, 2008).

Regarding these parameters in the roots, H_2O_2 content was much higher in both Co and Co+EE2 groups (both with similar values), while EE2 had similar values to the CTL. MDA content, however, was significantly higher for all treatments, being slightly higher in the coexposure than the individual exposures. Regarding the high MDA levels in the EE2 group, despite the values of H_2O_2 being similar to the CTL, this phenomenon has been previously reported by Christou et al. (2016), further implying that this hormone may be increasing other ROS levels, or inducing cellular damage through another pathway, such as nitro-oxidative stress (Corpas and Barroso, 2013). Quantification assays for the other ROS and reactive nitrogen species (RNS) would allow to test this hypothesis.

These results show that the coexposure was more deleterious to the plants than the single exposure, thus suggesting that EE2 does accentuate the negative effects triggered by the excess Co.

Since the increase in H_2O_2 levels can be associated to either a spontaneous formation, increased SOD activity or an insufficient removal by the other components of the AOX system (Sharma et al., 2012), these parameters were, therefore, evaluated. SOD activity decreased significantly in the Co treatment, in the aerial part, while for the other treatments, the levels were similar to the CTL. As to the roots, although the same pattern was visible, there were no significant differences detected between treatments. A reduction in this enzyme's activity was also present in *L. minor* exposed to Co (Begović et al., 2016). This may be due to an inactivation of particular SOD isoforms, since Co has affinity for complexes that possess Fe, Mn, Zn and Cu, possibly switching places with these metals and hence reducing the activity of enzymes possessing them, such as SOD (Chatterjee and Chatterjee, 2000). These results demonstrate that SOD activity was not responsible for the identified increases in H_2O_2 levels.

As to APX activity, it decreased substantially in both the EE2 and coexposure groups, in the shoots, not being substantially changed by Co single treatment. An increase in APX activity in response to Co has been reported in mustard (*Brassica campestris* L.) leaves (Sinha et al., 2012), however, the results from the EE2 treatment differ from the ones obtained for lettuce leaves by Adeel et al. (2018), where APX activity increased in plants exposed this hormone, although in this study higher concentrations were used (> 150 $\mu g.L^{-1}$). Nevertheless, APX's activity has been shown to be inhibited by other abiotic stresses, such as exposure to NaCl (de Queirós, 2012). Furthermore, the lower AsA/total ratio detected in the same organ in the coexposure treatment must have contributed to the observed decrease in this enzyme's activity, since it depends on the AsA pool to function (Soares et al., 2019).

GR activity followed the same pattern as APX for the shoots, with a decrease in both the EE2 and coexposure groups and a non-significant increase in the Co situation. Contrarily, an increase in GR activity has been detected in Indian mustard leaves exposed to Co (Karuppanapandian and Kim, 2013). In the roots, however, the coexposure led to significantly higher levels of this enzyme's activity, with similar values for the other treatments. These results differ from the ones obtained from the GR_{plast} gene expression as, in this case, expression increased for all treatments in the roots and

increased in the Co situation but decreased in the coexposure treatment in the shoots, indicating a post-transcriptional and/or post-translational regulation of this enzyme's activity.

Neither CAT nor DHAR showed significantly different activity levels in any treatment for roots and shoots. It has previously been suggested that CAT does not play a role in H_2O_2 removal from Co-induced stress (Karuppanapandian and Kim, 2013).

Pro levels in the roots showed a significant reduction in the coexposure treatment, with a tendency to decrease in Co and EE2's groups. This decrease supports the notion that the cellular damage observed in roots was not due to osmotic stress, and might be attributed to an increase in Pro catabolic enzymes' activity (Filippou et al., 2014). Furthermore, since Pro acts as a chelating agent, this decrease supports the aggravated effects of Co in the coexposure, like the increased LP degree.

GSH levels in the shoot increased substantially in the coexposure group, while the other treatments showed similar values to the CTL. The increased GR activity in the roots observed for this same treatment must have contributed to this phenomenon, since it would have increased the GSH pool, which would then be translocated to the shoots. In fact, GSH is known to be the main transport form of reduced sulfur in plants (Rennenberg et al., 1979; Foyer et al., 2001). This would also explain the decrease in GR activity detected in the shoots for this situation, since GSH had been imported from the roots and was no longer necessary for GR to increase its pool. In the roots, there was a drastic decrease in GSH levels in the EE2 group. In this case, the increased GST activity detected in the shoots would have required GSH to conjugate to EE2 (see below) and, as was the case for the coexposure group, GSH was translocated from the roots to be used in the shoots. The decrease in GR activity observed in the shoots in this case supports the results from the coexposure, as GR would not be necessary to increase the GSH pool in this organ, as this peptide would have been translocated from the roots.

In the aerial part of the plant, Co induced a higher total ascorbate (AsA+DHA) accumulation, whereas in the roots, only AsA's levels increased, resulting in a drastic increase in the AsA/DHA ratio. Since APX and DHAR's activity levels were not significantly altered in this treatment, it supports AsA's role as a non-enzymatic AOX. AsA, DHA, and total ascorbate levels have been demonstrated to increase in *Brassica juncea* L. leaves exposed to Co (Karuppanapandian and Kim, 2013). Plants

from the EE2 group showed similar levels to the CTL. In the coexposure, AsA, DHA, and total ascorbate levels were higher for the shoots, while only AsA and total ascorbate levels increased in the roots. Thus, while EE2 by itself did not elicit a response from the plant regarding this parameter, it did increase the response when applied together with Co.

The increased levels of both GSH and AsA in the shoots of plants from the coexposure group must have helped to cope with the Co present in this organ, which explains why SOD was no longer inhibited in this treatment, leading to higher H_2O_2 levels. Moreover, MDA levels were higher in this same situation, despite the increase in these AOXs' levels, which indicates that the raised GSH and AsA levels were not enough to prevent LP.

Despite the indications from the AOX system and oxidative stress levels that EE2 did not protect the plant against Co-induced stress, since the biometric parameters of the plants from the coexposure group reverted to values similar to the CTL's, the hypothesis that these plants' detoxification systems may play an important role in plant defense was further investigated.

4.4. Co and EE2's detoxification mechanisms

An essential mechanism through which plants deal with HMs- and xenobiotics-induced stresses is the synthesis of specific chelators, which prevent the binding of these toxic compounds to physiologically important proteins and facilitate their transport to vacuoles. Among these, MTs and PCs (generated from GSH) are important metal chelators. Furthermore, GST plays a major role in xenobiotics detoxification, by conjugating them to GSH (Labrou et al., 2015). In order to assess Co and EE2's impact on these chelators' synthesis, the transcript accumulation patterns for MTs, γ-ECS, PCS and GSTU's coding genes (with the same names) were evaluated.

In the shoots, plants from the Co group presented lower transcript levels for *MT2* and higher levels for *GSTU*, *PCS* and *γ-ECS*. In fact, a regulation at the transcription level of plant MTs by Co and an activation of PCS by this metal have been previously suggested (Yan et al., 2000; Yang et al., 2005). In the roots, the same plants showed higher mRNA levels for *MT1*, *MT2* and *MT4*. Such results clearly demonstrate that exposure to Co alone triggers a differential gene expression regulation in an organ-specific manner, where PCs play a more important role in shoot Co homeostasis than MT2, empowered

by an increased participation of γ-ECS, which provides GSH for PCs' synthesis. The increased shoot *GSTU* expression surely contributed towards the detoxification of toxic plant metabolites resulting from the increased ROS levels (Das and Roychoudhury, 2014), although the increase in GST activity detected for this situation and organ was not significant. Considering roots, the increased transcription of *MT1*, *MT2* and *MT4* was needed to counteract the increased levels of Co being absorbed by the plants by this organ. Such is perfectly understandable, since roots were the entry point of Co to the plant and, therefore, a protective measure was needed to prevent this HM to be transported to the shoots, where it would impair photosynthesis and other biosynthetic processes, thus threatening plant survival. Therefore, the quantification of the levels of this HM within the plant is needed to determine where the absorbed Co is most accumulated and to test this hypothesis.

As to the EE2 group, the aerial part of the plants demonstrated higher transcription for MT1 and GSTU's coding genes and a lower transcription for MT2's gene. The increased expression of *GSTU* is in accordance with its increased activity and may be a protective measure to conjugate the excess EE2 that was translocated to the shoots (Christou et al., 2016). Similarly, an increased expression in the *GST17* gene was detected in the leaves of *Medicago sativa* L. exposed to 10 $\mu g.L^{-1}$ EE2 (Christou et al., 2016). In the roots, *MT1* and *MT4*'s mRNA accumulation was increased in these plants, whereas *MT2*, *PCS* and *γ-ECS*'s transcription levels were decreased. This decrease in the *γ-ECS*'s expression could partially explain the drastic decrease in GSH levels registered in roots which, consequently, would have a negative impact on the synthesis of PCs (as this pseudopeptides are the result of the condensation of several GSH molecules), thus explaining the decreased transcription for *PCS*. Moreover, these results show that this hormone regulates MTs' genes' expressions, at least indirectly, in both organs. No information regarding the effects of estrogens on plant MT gene expression has been published yet, but a link between estrogen exposure and MTs regulation in animals has been supported by Werner et al. (2003).

Finally, plants from the coexposure treatment showed loss of expression for MT1, MT4, PCS and γ-ECS's coding genes in the shoots, with a decreased expression for GSTU's gene, which was opposite to the observed increase in GST activity for this organ, indicating post-transcriptional and/or post-translational regulation for this enzyme. In the roots of the same plants, *MT1* showed higher transcription levels, opposite to GSTU,

PCS and γ-ECS's genes, which expressions decreased. Comparing the results of the roots to those obtained for the same organ from the plants exposed solely to Co it is interesting to highlight a common response, which is the increased expression of *MT1*. This particular response strongly suggests that MT1-encoding genes may be Co-responsive, while the other MT-encoding genes may be regulated by other factors other than Co, like the enhanced ROS (Hassinen et al., 2011). The decreased *PCS* expression may be partially explained by the decrease in Pro content observed in this treatment, as Pro facilitates PCs formation by maintaining a more favorable reduced environment (Siripornadulsil et al., 2002). Again, the comparison between the Co levels in roots from these plants and the ones from the Co single exposure would allow to test this hypothesis: if such levels were similar or higher in the Co-treated plants, then it would indicate that MT1 sufficed for root Co homeostasis; if the Co levels in the Co-treated plants were lower, that would indicate that Co was being translocated to the aboveground part of the plant, thus explaining the increased MDA levels detected therein.

Concluding Remarks

This research provided novel information concerning the effects of EE2 in plants' AOX system and detoxifying mechanisms and has evidenced differential responses from these organisms when exposed to both EE2 and Co, or to just one of these pollutants. Furthermore, it demonstrated that MTs- and PCs-related genes can have their transcription influenced by an exposure to these contaminants.

Regarding the harmful effects induced by Co, it was demonstrated that plants exposed to this HM showed a decreased SOD activity and higher levels of ROS, which led to an increased LP, compromising cell membranes, reduced biomass and starch accumulation, induced chlorosis and necrotic spots in the leaves. To counteract these effects, the plant invested in the protective role of AsA, MTs and PCs, with MTs encoding genes' expression being upregulated in the roots, *GSTU*, *γ-ECS* and *PCS*'s increased in the shoots and GR_{plast}'s in both roots and shoots.

Macroscopically, EE2 stimulated shoot growth, indicating a stimulatory effect. However, it caused some negative effects on the plant's physiology, inducing LP, depleting GSH levels, downregulating γ-*ECS*, *PCS* and *MT2*'s expression and inhibiting APX and GR's

activity. To deal with the presence of this contaminant, the plant responded by increasing GST's activity and *GSTU*, *MT1*, *MT4* and GR_{plast}'s expression.

When analyzing the results obtained in the coexposure, at first glance, EE2 appeared to ameliorate the effects of Co-induced stress, as the biometric values were similar to the CTL's. However, the analysis of some oxidative stress indicators demonstrated that, more often than not, EE2 aggravated the effects caused by Co, increasing ROS levels, decreasing Pro levels in the roots and APX and GR's activities in the shoots and inhibiting gene expression for molecules involved in the detoxification process (MTs, PCS, GSTU). Still, GSH and AsA levels and GST activity were stimulated in this situation, which is most likely how the plants managed to revert to biometric levels close to those of the CTL.

A summary table containing all results obtained in this work can be found in Supplemental Data 3.

More studies are necessary to understand the modes of action of EE2 on plant physiology, as well as how a coexposure with this hormone and a HM such as Co can impact crops in a longer term, namely in the fruit production phase, to assess whether this situation is beneficial or not where yield and productivity are concerned.

Future Perspectives

This study provided some new insights on Co and EE2's effects on plants, as well as on the defense and detoxifying mechanisms these pollutants elicit from these sessile organisms, both in individual and combined exposures. However, some raised hypothesis need further exploration in subsequent studies:

- Quantification of both compounds in plant tissues (roots and shoots) to understand if the detected responses are consistent with the levels of the pollutants in these organs;
- Evaluation of the levels of other ROS and RNS to comprehend which ones are more connected to the observed membrane damage;
- Reassessment of photosynthetic pigments content with a different protocol, so that the results obtained represent the entire leaf;

- Analysis of MTs genes' expression through qPCR, for a sounder profile on these genes' transcript accumulation levels in response to these contaminants;
- Assessment of γ-ECS and PCS' activities, to see if they correspond to their genes' transcription levels;
- Evaluation of the activity of enzymes responsible for providing precursor molecules to GSH synthesis, such as glutamine synthetase (GS, EC 6.3.1.2);
- Quantification of other metal nutrients whose absorption by the plant may have been affected by Co, such as Fe and Cu.

References

Adeel M, Song X, Wang Y, Francis D, Yang Y (2017) Environmental impact of estrogens on human, animal and plant life: A critical review. Environ Int **99:** 107-119

Adeel M, Yang Y, Wang Y, Song X, Ahmad MA, Rogers HJ (2018) Uptake and transformation of steroid estrogens as emerging contaminants influence plant development. Environ Pollut **243:** 1487-1497

Adriano DC (2013) Trace elements in the terrestrial environment. Springer Science & Business Media

Aebi H (1984) Catalase in vitro. Method Enzymol **105:** 121-126

Akashi K, Nishimura N, Ishida Y, Yokota A (2004) Potent hydroxyl radical-scavenging activity of drought-induced type-2 metallothionein in wild watermelon. Biochem Biophys Res Commun **323:** 72-78

Akinci IE, Akinci S (2010) Effect of chromium toxicity on germination and early seedling growth in melon (*Cucumis melo* L.). Afr J Biotechnol **9:** 4589-4594

Alexieva V, Sergiev I, Mapelli S, Karanov E (2001) The effect of drought and ultraviolet radiation on growth and stress markers in pea and wheat. Plant Cell Environ **24:** 1337-1344

Ali B, Hayat S, Hayat Q, Ahmad A (2010) Cobalt stress affects nitrogen metabolism, photosynthesis and antioxidant system in chickpea (*Cicer arietinum* L.). J Plant Interact **5:** 223-231

Almeida Â, Silva MG, Soares AM, Freitas R (2020) Concentrations levels and effects of 17alpha-Ethinylestradiol in freshwater and marine waters and bivalves: A review. Environ Res **185:** 109316

An J, Zhou Q, Sun F, Zhang L (2009) Ecotoxicological effects of paracetamol on seed germination and seedling development of wheat (*Triticum aestivum* L.). J Hazard Mater **169:** 751-757

Anjum NA, Hasanuzzaman M, Hossain MA, Thangavel P, Roychoudhury A, Gill SS, Rodrigo MAM, Adam V, Fujita M, Kizek R, Duarte AC, Pereira E, Ahmad I (2015) Jacks of metal/metalloid chelation trade in plants—an overview. Front Plant Sci **6**

Anwar R, Fatima T, Mattoo A (2019) Tomatoes: A model crop of Solanaceous plants. Oxford Research Encyclopedia of Environmental Science. Oxford University Press

Aris AZ, Shamsuddin AS, Praveena SM (2014) Occurrence of 17α-ethynylestradiol (EE2) in the environment and effect on exposed biota: a review. Environ Int **69:** 104-119

Arnon S, Dahan O, Elhanany S, Cohen K, Pankratov I, Gross A, Ronen Z, Baram S, Shore LS (2008) Transport of Testosterone and Estrogen from Dairy-Farm Waste Lagoons to Groundwater. Environ Sci Technol **42:** 5521-5526

Bajguz A, Hayat S (2009) Effects of brassinosteroids on the plant responses to environmental stresses. Plant Physiol Biochem **47:** 1-8

Bakkaus E, Gouget B, Gallien JP, Khodja H, Carrot F, Morel JL, Collins R (2005) Concentration and distribution of cobalt in higher plants: The use of micro-PIXE spectroscopy. Nucl Instrum Meth B **231:** 350-356

Bakshi S, Banik C, He Z (2018) The impact of heavy metal contamination on soil health, Vol 2

Bartrons M, Peñuelas J (2017) Pharmaceuticals and Personal-Care Products in Plants. Trends Plant Sci **22:** 194-203

Bates LS, Waldren RP, Teare I (1973) Rapid determination of free proline for water-stress studies. Plant Soil **39:** 205-207

Beauchamp C, Fridovich I (1971) Superoxide dismutase: improved assays and an assay applicable to acrylamide gels. Anal Biochem **44:** 276-287

Begović L, Mlinarić S, Dunić JA, Katanić Z, Lončarić Z, Lepeduš H, Cesar V (2016) Response of *Lemna minor* L. to short-term cobalt exposure: The effect on

photosynthetic electron transport chain and induction of oxidative damage. Aquat Toxicol **175:** 117-126

Bircher S (2011) Phytoremediation of natural and synthetic steroid growth promoters used in livestock production by riparian buffer zone plants. The University of Iowa

Blume H, Brümmer G, Horn R, Kandeler E, Kögel-Knabner I, Kretzschmar R, Stahr K, Wilke B (2010) Scheffer/Schachtschabel–Soil Science Textbook (Lehrbuch der Bodenkunde). Spektrum Akademischer Verlag, Heidelberg, Germany

Brkljačić JM, Samardžić JT, Timotijević GS, Maksimović VR (2004) Expression analysis of buckwheat (*Fagopyrum esculentum* Moench) metallothionein-like gene (*MT3*) under different stress and physiological conditions. J Plant Physiol **161:** 741-746

Bulda O, Rassadina V, Alekseichuk H, Laman N (2008) Spectrophotometric measurement of carotenes, xanthophylls, and chlorophylls in extracts from plant seeds. Russ J Plant Physl+ **55:** 544-551

Caldeira C (2019) Portugal exporta 77% da sua produção de tomate transformado. Agricultura e Mar Actual,

Cardoso O, Porcher J-M, Sanchez W (2014) Factory-discharged pharmaceuticals could be a relevant source of aquatic environment contamination: Review of evidence and need for knowledge. Chemosphere **115:** 20-30

Chaoui A, El Ferjani E (2013) β-Estradiol protects embryo growth from heavy-metal toxicity in germinating lentil seeds. J Plant Growth Regul **32:** 636-645

Chatterjee J, Chatterjee C (2000) Phytotoxicity of cobalt, chromium and copper in cauliflower. Environmental Pollution **109:** 69-74

Chatterjee J, Chatterjee C (2003) Management of phytotoxicity of cobalt in tomato by chemical measures. Plant Sci **164:** 793-801

Chaturvedi R, Favas PJC, Pratas J, Varun M, Paul MS (2018) Effect of *Glomus mosseae* on accumulation efficiency, hazard index and antioxidant defense mechanisms in tomato under metal(loid) Stress. Int J Phytoremediation **20:** 885-894

Chen Q, Wu Z, Liu J (2011) Ecotoxicity of chloramphenicol and Hg acting on the root elongation of crops in North China. Int J Environ Res **5:** 909-916

Christou A, Antoniou C, Christodoulou C, Hapeshi E, Stavrou I, Michael C, Fatta-Kassinos D, Fotopoulos V (2016) Stress-related phenomena and detoxification

mechanisms induced by common pharmaceuticals in alfalfa (*Medicago sativa* L.) plants. Sci Total Environ **557:** 652-664

Cobbett C, Goldsbrough P (2002) Phytochelatins and metallothioneins: roles in heavy metal detoxification and homeostasis. Annu Rev Plant Biol **53:** 159-182

Connell DW, Qiming JY, Verma V (2016) Influence of exposure time on toxicity—An overview. Toxicology **355:** 49-53

Corpas FJ, Barroso JB (2013) Nitro-oxidative stress vs oxidative or nitrosative stress in higher plants. New Phytol **199:** 633-635

Das K, Roychoudhury A (2014) Reactive oxygen species (ROS) and response of antioxidants as ROS-scavengers during environmental stress in plants. Front Environ Sci **2:** 53

De La Torre Roche R, Pagano L, Majumdar S, Eitzer BD, Zuverza-Mena N, Ma C, Servin AD, Marmiroli N, Dhankher OP, White JC (2018) Co-exposure of imidacloprid and nanoparticle Ag or CeO2 to *Cucurbita pepo* (zucchini): Contaminant bioaccumulation and translocation. NanoImpact **11:** 136-145

de Pinto MC, De Gara L (2004) Changes in the ascorbate metabolism of apoplastic and symplastic spaces are associated with cell differentiation. J Exp Bot **55:** 2559-2569

de Queirós MFMA (2012) Tolerância à salinidade em linha celular de *Solanum tuberosum* L. - estudo bioquímico, proteómico e ultraestrutural. FCUP, Porto

Donahue JL, Okpodu CM, Cramer CL, Grabau EA, Alscher RG (1997) Responses of antioxidants to paraquat in pea leaves (relationships to resistance). Plant Physiol **113:** 249-257

Dussault ÈB, Balakrishnan VK, Borgmann U, Solomon KR, Sibley PK (2009) Bioaccumulation of the synthetic hormone 17α-ethinylestradiol in the benthic invertebrates *Chironomus tentans* and *Hyalella azteca*. Ecotox Environ Safe **72:** 1635-1641

Dzieweczynski TL, Hentz KB, Logan B, Hebert OL (2014) Chronic exposure to 17α-ethinylestradiol reduces behavioral consistency in male Siamese fighting fish. Behaviour **151:** 633-651

Ebele AJ, Abou-Elwafa Abdallah M, Harrad S (2017) Pharmaceuticals and personal care products (PPCPs) in the freshwater aquatic environment. Emerg Contam **3:** 1-16

Emamverdian A, Ding Y, Mokhberdoran F, Xie Y (2015) Heavy metal stress and some mechanisms of plant defense response. Sci World J

Erdal S (2009) Effects of mammalian sex hormones on antioxidant enzyme activities, H_2O_2 content and lipid peroxidation in germinating bean seeds. J Fac Agr **40:** 79-85

Erdal S (2012) Alleviation of salt stress in wheat seedlings by mammalian sex hormones. J Sci Food Agric **92:** 1411-1416

Erdal S, Dumlupinar R (2011) Mammalian sex hormones stimulate antioxidant system and enhance growth of chickpea plants. Acta Physiol Plant **33:** 1011-1017

Erickson BE (2002) Analyzing the ignored environmental contaminants. Environ Sci Technol **36:** 140A-145A

Farago ME, Mullen WA (1979) Plants which accumulate metals. Part IV. A possible copper-proline complex from the roots of *Armeria maritima*. Inorg Chim Acta **32:** L93-L94

Filippou P, Bouchagier P, Skotti E, Fotopoulos V (2014) Proline and reactive oxygen/nitrogen species metabolism is involved in the tolerant response of the invasive plant species *Ailanthus altissima* to drought and salinity. Environ Exp Bot **97:** 1-10

Foyer CH, Noctor G (2008) Redox Regulation in Photosynthetic Organisms: Signaling, Acclimation, and Practical Implications. Antioxid Redox Sign **11:** 861-905

Foyer CH, Theodoulou FL, Delrot S (2001) The functions of inter- and intracellular glutathione transport systems in plants. Trends Plant Sci **6:** 486-492

Freisinger E (2011) Structural features specific to plant metallothioneins. J Biol Inorg Chem **16:** 1035-1045

Froehner S, Machado KS, Stefan E, Bleninger T, da Rosa EC, de Castro Martins C (2012) Occurrence of selected estrogens in mangrove sediments. Mar Pollut Bull **64:** 75-79

Gadd JB, Tremblay LA, Northcott GL (2010) Steroid estrogens, conjugated estrogens and estrogenic activity in farm dairy shed effluents. Environ Pollut **158:** 730-736

Gál J, Hursthouse A, Tatner P, Stewart F, Welton R (2008) Cobalt and secondary poisoning in the terrestrial food chain: Data review and research gaps to support risk assessment. Environ Int **34:** 821-838

Genişel M, Türk H, Erdal S, Genç E, Terzi İ, Demir Y (2015) Ameliorative role of β-estradiol against lead-induced oxidative stress and genotoxic damage in germinating wheat seedlings. Turk J Bot **39**

Gerszberg A, Hnatuszko-Konka K, Kowalczyk T, Kononowicz AK (2015) Tomato (*Solanum lycopersicum* L.) in the service of biotechnology. Plant Cell Tiss Org **120:** 881-902

Gill SS, Tuteja N (2010) Reactive oxygen species and antioxidant machinery in abiotic stress tolerance in crop plants. Plant Physiol Bioch **48:** 909-930

Gillespie KM, Ainsworth EA (2007) Measurement of reduced, oxidized and total ascorbate content in plants. Nat Protoc **2:** 871-874

Gopal R, Dube B, Sinha P, Chatterjee C (2003) Cobalt toxicity effects on growth and metabolism of tomato. Commun Soil Sci Plan **34:** 619-628

Hare P, Cress W (1997) Metabolic implications of stress-induced proline accumulation in plants. Plant Growth Regul **21:** 79-102

Hasanuzzaman M, Nahar K, Anee TI, Fujita M (2017) Glutathione in plants: biosynthesis and physiological role in environmental stress tolerance. Physiol Mol Biol Pla **23:** 249-268

Hassinen VH, Tervahauta AI, Schat H, Kärenlampi SO (2011) Plant metallothioneins – metal chelators with ROS scavenging activity? Plant Biol **13:** 225-232

Hayat S, Hayat Q, Alyemeni MN, Wani AS, Pichtel J, Ahmad A (2012) Role of proline under changing environments. Plant Signal Behav **7:** 1456-1466

Heath RL, Packer L (1968) Photoperoxidation in isolated chloroplasts: I. Kinetics and stoichiometry of fatty acid peroxidation. Arch Biochem Biophys **125:** 189-198

Hurtado C, Domínguez C, Pérez-Babace L, Cañameras N, Comas J, Bayona JM (2016) Estimate of uptake and translocation of emerging organic contaminants from irrigation water concentration in lettuce grown under controlled conditions. J Hazard Mater **305:** 139-148

Ishikawa T, Shigeoka S (2008) Recent Advances in Ascorbate Biosynthesis and the Physiological Significance of Ascorbate Peroxidase in Photosynthesizing Organisms. Biosci Biotechnol Biochem **72:** 1143-1154

Janeczko A, Budziszewska B, Skoczowski A, Dybała M (2008) Specific binding sites for progesterone and 17beta-estradiol in cells of Triticum aestivum L. Acta Biochimica Polonica **55:** 707-711

Janeczko A, Skoczowski A (2005) Mammalian sex hormones in plants. Folia Histochem Cytobiol **43:** 71-79

Jayakumar K, Jaleel CA, Azooz M (2008) Impact of cobalt on germination and seedling growth of *Eleusine coracana* L. and *Oryza sativa* L. under hydroponic culture. G J Mol Sci **3:** 18-20

Joshi R, Pareek A, Singla-Pareek SL (2016) Plant metallothioneins: classification, distribution, function, and regulation. Plant Metal Interaction. Elsevier, pp 239-261

Karnjanapiboonwong A, Chase DA, Cañas JE, Jackson WA, Maul JD, Morse AN, Anderson TA (2011) Uptake of 17α-ethynylestradiol and triclosan in pinto bean, *Phaseolus vulgaris*. Ecotox Environ Safe **74:** 1336-1342

Karuppanapandian T, Kim W (2013) Cobalt-induced oxidative stress causes growth inhibition associated with enhanced lipid peroxidation and activates antioxidant responses in Indian mustard (*Brassica juncea* L.) leaves. Acta Physiol Plant **35:** 2429-2443

Khan A, Khan S, Khan MA, Qamar Z, Waqas M (2015) The uptake and bioaccumulation of heavy metals by food plants, their effects on plants nutrients, and associated health risk: a review. Environ Sci Pollut R **22:** 13772-13799

Kimura S, Sinha N (2008) Tomato (*Solanum lycopersicum*): a model fruit-bearing crop. CSH Protoc **2008:** pdb. emo105

Labrou NE, Papageorgiou AC, Pavli O, Flemetakis E (2015) Plant GSTome: structure and functional role in xenome network and plant stress response. Curr Opin Biotechnol **32:** 186-194

Lago-Vila M, Arenas-Lago D, Rodríguez-Seijo A, Andrade Couce M, Vega F (2015) Cobalt, chromium and nickel contents in soils and plants from a serpentinite quarry. Solid earth **6:** 323-335

Larcher S, Yargeau V (2013) Biodegradation of 17α-ethinylestradiol by heterotrophic bacteria. Environ Pollut **173:** 17-22

Leszczyszyn OI, Imam HT, Blindauer CA (2013) Diversity and distribution of plant metallothioneins: a review of structure, properties and functions. Metallomics **5:** 1146-1169

Li W, Khan MA, Yamaguchi S, Kamiya Y (2005) Effects of heavy metals on seed germination and early seedling growth of *Arabidopsis thaliana*. Plant Growth Regul **46:** 45-50

Liao X-Y, Gong X-G, Zhang L-L, Cassidy DP (2021) Micro-distribution of arsenic and polycyclic aromatic hydrocarbons and their interaction in *Pteris vittata* L. Environ Pollut **285:** 117250

Lima DLD, Calisto V, Esteves VI (2011) Adsorption behavior of 17α-ethynylestradiol onto soils followed by fluorescence spectral deconvolution. Chemosphere **84:** 1072-1078

Lopez-Luna J, Gonzalez-Chavez M, Esparza-Garcia F, Rodriguez-Vazquez R (2009) Toxicity assessment of soil amended with tannery sludge, trivalent chromium and hexavalent chromium, using wheat, oat and sorghum plants. J Hazard Mater **163:** 829-834

Løvdal T, Lillo C (2009) Reference gene selection for quantitative real-time PCR normalization in tomato subjected to nitrogen, cold, and light stress. Anal Biochem **387:** 238-242

Lwalaba JLW, Zvobgo G, Fu L, Zhang X, Mwamba TM, Muhammad N, Mundende RPM, Zhang G (2017) Alleviating effects of calcium on cobalt toxicity in two barley genotypes differing in cobalt tolerance. Ecotox Environ Safe **139:** 488-495

Mahey S, Kumar R, Sharma M, Kumar V, Bhardwaj R (2020) A critical review on toxicity of cobalt and its bioremediation strategies. SN Appl Sci **2:** 1279

Margoshes M, Vallee BL (1957) A cadmium protein from equine kidney cortex. Journal of the American Chemical Society **79:** 4813-4814

Martins M, Sousa B, Lopes J, Soares C, Machado J, Carvalho S, Fidalgo F, Teixeira J (2020) Diclofenac shifts the role of root glutamine synthetase and glutamate dehydrogenase for maintaining nitrogen assimilation and proline production at the expense of shoot carbon reserves in *Solanum lycopersicum* L. Environ Sci Pollut Res **27:** 29130-29142

Martins M, Sousa B, Lopes J, Soares C, Machado J, Carvalho S, Fidalgo F, Teixeira J (2020) Diclofenac shifts the role of root glutamine synthetase and glutamate dehydrogenase for maintaining nitrogen assimilation and proline production at the expense of shoot carbon reserves in *Solanum lycopersicum* L. Environ Sci Pollut R **27:** 29130-29142

Merrifield ME, Ngu T, Stillman MJ (2004) Arsenic binding to *Fucus vesiculosus* metallothionein. Biochem Biophys Res Commun **324:** 127-132

Mittler R (2006) Abiotic stress, the field environment and stress combination. Trends Plant Sci **11:** 15-19

Montagner CC, Jardim WF (2011) Spatial and seasonal variations of pharmaceuticals and endocrine disruptors in the Atibaia River, São Paulo State (Brazil). J Brazil Chem Soc **22:** 1452-1462

Monteiro SC, Boxall AB (2010) Occurrence and fate of human pharmaceuticals in the environment. Rev Environ Contam T**:** 53-154

Murshed R, Lopez-Lauri F, Sallanon H (2008) Microplate quantification of enzymes of the plant ascorbate–glutathione cycle. Anal Biochem **383:** 320-322

Nagajyoti PC, Lee KD, Sreekanth T (2010) Heavy metals, occurrence and toxicity for plants: a review. Environ Chem Lett **8:** 199-216

Nguyen TPL, Mula L, Cortignani R, Seddaiu G, Dono G, Virdis SG, Pasqui M, Roggero PP (2016) Perceptions of present and future climate change impacts on water availability for agricultural systems in the western Mediterranean region. Water **8:** 523

Nnorom IC, Osibanjo O (2009) Heavy metal characterization of waste portable rechargeable batteries used in mobile phones. Int J Environ Sci Te **6:** 641-650

Noctor G, Mhamdi A, Chaouch S, Han Y, Neukermans J, Marquez-Garcia B, Queval G, Foyer CH (2012) Glutathione in plants: an integrated overview. Plant Cell Environ **35:** 454-484

Noctor G, Reichheld J-P, Foyer CH (2018) ROS-related redox regulation and signaling in plants. Semin Cell Dev Biol **80:** 3-12

Oladeji S, Saeed M (2015) Assessment of cobalt levels in wastewater, soil and vegetable samples grown along Kubanni stream channels in Zaria, Kaduna State, Nigeria. Afr J Environ Sci Technol **9:** 765-772

Pan M, Chu L (2016) Phytotoxicity of veterinary antibiotics to seed germination and root elongation of crops. Ecotox Environ Safe **126:** 228-237

Panagos P, Van Liedekerke M, Yigini Y, Montanarella L (2013) Contaminated sites in Europe: review of the current situation based on data collected through a European network. J Environ Public Health **2013**

Pescod MB (1992) Wastewater treatment and use in agriculture - FAO irrigation and drainage paper 47.

R. Benatti M, Yookongkaew N, Meetam M, Guo WJ, Punyasuk N, AbuQamar S, Goldsbrough P (2014) Metallothionein deficiency impacts copper accumulation and redistribution in leaves and seeds of *Arabidopsis*. New Phytol **202:** 940-951

Ren Y, Liu Y, Chen H, Li G, Zhang X, Zhao J (2012) Type 4 metallothionein genes are involved in regulating Zn ion accumulation in late embryo and in controlling early seedling growth in *Arabidopsis*. Plant Cell Environ **35:** 770-789

Rennenberg H, Schmitz K, Bergmann L (1979) Long-distance transport of sulfur in *Nicotiana tabacum*. Planta **147:** 57-62

Ribeiro C, Tiritan ME, Rocha E, Rocha MJ (2009) Seasonal and spatial distribution of several endocrine-disrupting compounds in the Douro River Estuary, Portugal. Arch Environ Con Tox **56:** 1-11

Roosens NH, Bernard C, Leplae R, Verbruggen N (2004) Evidence for copper homeostasis function of metallothionein (MT3) in the hyperaccumulator *Thlaspi caerulescens*. FEBS Lett **577:** 9-16

Rzymski P, Drewek A, Klimaszyk P (2017) Pharmaceutical pollution of aquatic environment: an emerging and enormous challenge. Limnol Rev **17:** 97-107

Saaristo M, Craft JA, Lehtonen KK, Lindström K (2009) Sand goby (*Pomatoschistus minutus*) males exposed to an endocrine disrupting chemical fail in nest and mate competition. Horm Behav **56:** 315-321

Sadutto D, Andreu V, Ilo T, Akkanen J, Picó Y (2021) Pharmaceuticals and personal care products in a Mediterranean coastal wetland: Impact of anthropogenic and spatial factors and environmental risk assessment. Environ Pollut **271:** 116353

Salgado R, Noronha J, Oehmen A, Carvalho G, Reis M (2010) Analysis of 65 pharmaceuticals and personal care products in 5 wastewater treatment plants in Portugal using a simplified analytical methodology. Water Sci Technol **62:** 2862-2871

Sauvé S, Desrosiers M (2014) A review of what is an emerging contaminant. Chem Cent J **8:** 15

Sharma P, Jha AB, Dubey RS, Pessarakli M (2012) Reactive Oxygen Species, Oxidative Damage, and Antioxidative Defense Mechanism in Plants under Stressful Conditions. J Bot

Sharma SS, Schat H, Vooijs R (1998) In vitro alleviation of heavy metal-induced enzyme inhibition by proline. Phytochemistry **49:** 1531-1535

Simons R, Grinwich D (1989) Immunoreactive detection of four mammalian steroids in plants. Can J Botany **67:** 288-296

Sinha P, Khurana N, Nautiyal N (2012) Induction of oxidative stress and antioxidant enzymes by excess cobalt in mustard. J Plant Nutr **35:** 952-960

Siripornadulsil S, Traina S, Verma DPS, Sayre RT (2002) Molecular Mechanisms of Proline-Mediated Tolerance to Toxic Heavy Metals in Transgenic Microalgae. Plant Cell **14:** 2837-2847

Soares C, Branco-Neves S, de Sousa A, Azenha M, Cunha A, Pereira R, Fidalgo F (2018) SiO_2 nanomaterial as a tool to improve *Hordeum vulgare* L. tolerance to nano-NiO stress. Sci Total Environ **622:** 517-525

Soares C, Branco-Neves S, de Sousa A, Pereira R, Fidalgo F (2016) Ecotoxicological relevance of nano-NiO and acetaminophen to *Hordeum vulgare* L.: Combining standardized procedures and physiological endpoints. Chemosphere **165:** 442-452

Soares C, Carvalho MEA, Azevedo RA, Fidalgo F (2019) Plants facing oxidative challenges—A little help from the antioxidant networks. Environ Exp Bot **161:** 4-25

Soares C, Pereira R, Spormann S, Fidalgo F (2019) Is soil contamination by a glyphosate commercial formulation truly harmless to non-target plants?–Evaluation of oxidative damage and antioxidant responses in tomato. Environ Pollut **247:** 256-265

Speranza A, Crosti P, Malerba M, Stocchi O, Scoccianti V (2011) The environmental endocrine disruptor, bisphenol A, affects germination, elicits stress response and alters steroid hormone production in kiwifruit pollen. Plant Biology **13:** 209-217

Sree KS, Keresztes Á, Mueller-Roeber B, Brandt R, Eberius M, Fischer W, Appenroth K-J (2015) Phytotoxicity of cobalt ions on the duckweed *Lemna minor*–Morphology, ion uptake, and starch accumulation. Chemosphere **131:** 149-156

Suzuki N, Rivero RM, Shulaev V, Blumwald E, Mittler R (2014) Abiotic and biotic stress combinations. New Phytologist **203:** 32-43

Taiz L, Zeiger E, Møller IM, Murphy A (2015) Plant Physiology and Development. Sinauer Associates Incorporated

Tarkowská D (2019) Plants are capable of synthesizing animal steroid hormones. Molecules **24:** 2585

Tausz M, Šircelj H, Grill D (2004) The glutathione system as a stress marker in plant ecophysiology: is a stress-response concept valid? J Exp Bot **55:** 1955-1962

Teixeira J, de Sousa A, Azenha M, Moreira JT, Fidalgo F, Silva AF, Faria JL, Silva AM (2011) *Solanum nigrum* L. weed plants as a remediation tool for metalaxyl-polluted effluents and soils. Chemosphere **85:** 744-750

Tosin R, Pôças I, Novo H, Teixeira J, Fontes N, Graça A, Cunha M (2021) Assessing predawn leaf water potential based on hyperspectral data and pigment's concentration of *Vitis vinifera* L. in the Douro Wine Region. Sci Hortic-Amsterdam **278:** 109860

Wang S, Zhu Z, He J, Yue X, Pan J, Wang Z (2018) Steroidal and phenolic endocrine disrupting chemicals (EDCs) in surface water of Bahe River, China: Distribution, bioaccumulation, risk assessment and estrogenic effect on *Hemiculter leucisculus*. Environ Pollut **243:** 103-114

Wang Y-M, Yang Q, Xu H, Liu Y-J, Yang H-L (2020) Physiological and transcriptomic analysis provide novel insight into cobalt stress responses in willow. Sci Rep-UK **10:** 2308

Werner J, Wautier K, Evans RE, Baron CL, Kidd K, Palace V (2003) Waterborne ethynylestradiol induces vitellogenin and alters metallothionein expression in lake trout (*Salvelinus namaycush*). Aquat Toxicol **62:** 321-328

Woodard TL, Thomas RJ, Xing B (2003) Potential for phytoextraction of cobalt by tomato. Commun Soil Sci Plan **34:** 645-654

Wu Z-z, Zhang Y-x, Yang J-y, Zhou Y, Wang C-q (2021) Effect of Vanadium on Testa, Seed Germination, and Subsequent Seedling Growth of Alfalfa (*Medicago sativa* L.). J Plant Growth Regul **40:** 1566-1578

Wuana RA, Okieimen FE (2011) Heavy metals in contaminated soils: a review of sources, chemistry, risks and best available strategies for remediation. Int Sch Res Notices **2011**

Yadav S (2010) Heavy metals toxicity in plants: an overview on the role of glutathione and phytochelatins in heavy metal stress tolerance of plants. S Afr J Bot **76:** 167-179

Yan S-L, Tsay C-C, Chen Y-R (2000) Isolation and characterization of phytochelatin synthase in rice seedlings. Proc Natl Sci Counc Republic China B Life Sci **24:** 202-206

Yang XE, JIN XF, Feng Y, Islam E (2005) Molecular mechanisms and genetic basis of heavy metal tolerance/hyperaccumulation in plants. J Integr Plant Biol **47:** 1025-1035

Yang Z, Wu Y, Li Y, Ling H-Q, Chu C (2009) OsMT1a, a type 1 metallothionein, plays the pivotal role in zinc homeostasis and drought tolerance in rice. Plant Mol Biol **70:** 219-229

Ye S, Zeng G, Wu H, Zhang C, Liang J, Dai J, Liu Z, Xiong W, Wan J, Xu P (2017) Co-occurrence and interactions of pollutants, and their impacts on soil remediation—a review. Crit Rev Env Sci Tec **47:** 1528-1553

Young IJ, Knights BA, Hillman JR (1977) Oestradiol and its biosynthesis in *Phaseolus vulgaris* L. Nature **267:** 429-429

Zar J (1996) Biostatistical analysis. Vol 662, Prentice Hall, New Jersey, p 256

Zenker A, Cicero MR, Prestinaci F, Bottoni P, Carere M (2014) Bioaccumulation and biomagnification potential of pharmaceuticals with a focus to the aquatic environment. J Environ Manage **133:** 378-387

Zimeri AM, Dhankher OP, McCaig B, Meagher RB (2005) The Plant MT1 Metallothioneins are Stabilized by Binding Cadmiums and are Required for Cadmium Tolerance and Accumulation. Plant Mol Biol **58:** 839-855

Supplemental Data

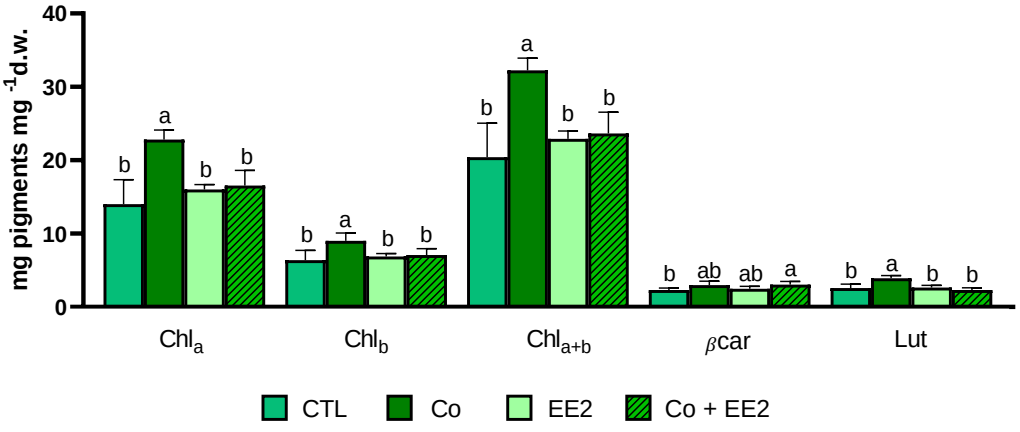

Supplemental Data 1 – Pigment concentrations expressed in mg per mg of dry weight in leaf disks of *S. lycopersicum* plants grown for 30 days in vermiculite:perlite (1:1), watered with: nutrient medium (CTL), nutrient medium supplemented with 50 µM Co (Co), nutrient medium supplemented with 500 ng.L^{-1} EE2 (EE2) or nutrient medium supplemented with both Co and EE2 (Co+EE2), in their respective concentrations. Different letters above bars represent significant differences (according to the Tukey test) at $p \leq 0.05$. Chl$_a$: Chlorophyl a; Chl$_b$: Chlorophyl b; Chl$_{a+b}$: total chlorophyl; βcar: βCarotene; Lut: lutein.

Supplemental Data 2 – Total, reduced and oxidized ascorbate levels and ratios in the shoots and roots of *S. lycopersicum* plants grown for 30 days in vermiculite:perlite (1:1), watered with: nutrient medium (CTL), nutrient medium supplemented with 50 µM Co (Co), nutrient medium supplemented with 500 ng.L^{-1} EE2 (EE2) or nutrient medium supplemented with both Co and EE2 (Co+EE2), in their respective concentrations. For simplicity, reduced AsA was termed AsA. Results are expressed as mean (µmol g^{-1} f. w.) ± SD. Different letters next to the values represent significant differences (according to the Tukey test) at $p \leq 0.05$.

Shoots						
	Total	**AsA**	**DHA**	**AsA/total**	**DHA/total**	**AsA/DHA**
CTL	0.31 ± 0.03 c	0.21 ± 0.03 b	0.10 ± 0.02 b	0.67 ± 0.07 a	0.33 ± 0.07 a	2.12 ± 0.70 a
Co	0.47 ± 0.09 b	0.29 ± 0.06 b	0.18 ± 0.09 b	0.62 ± 0.14 ab	0.38 ± 0.14 ab	1.88 ± 1.14 a
EE2	0.37 ± 0.07 bc	0.21 ± 0.04 b	0.16 ± 0.04 b	0.57 ± 0.02 ab	0.43 ± 0.02 ab	1.31 ± 0.10 a
Co+EE2	0.96 ± 0.02 a	0.44 ± 0.03 a	0.52 ± 0.06 a	0.46 ± 0.05 b	0.54 ± 0.05 b	0.86 ± 0.17 a
Roots						
	Total	**AsA**	**DHA**	**AsA/total**	**DHA/total**	**AsA/DHA**
CTL	0.78 ± 0.07 b	0.11 ± 0.01 c	0.67 ± 0.06 a	0.14 ± 0.01 b	0.86 ± 0.01 a	0.16 ± 0.01 b
Co	0.85 ± 0.11 ab	0.35 ± 0.07 ab	0.50 ± 0.05 a	0.41 ± 0.03 a	0.60 ± 0.03 b	0.68 ± 0.07 a
EE2	0.78 ± 0.09 b	0.13 ± 0.01 bc	0.65 ± 0.07 a	0.17 ± 0.01 b	0.83 ± 0.01 a	0.21 ± 0.01 b
Co+EE2	1.22 ± 0.25 a	0.55 ± 0.17 a	0.67 ± 0.08 a	0.45 ± 0.05 a	0.55 ± 0.05 b	0.82 ± 0.15 a

Supplemental Data 3 - Summary of the obtained results. ↑ - increase; ↓ - decrease; ↓↓ - loss of expression; **—** - No changes; **-** - negative effect; **+** - additive or synergistic effect; ○ - no effect.

	When compared to:	CTL						Co		EE2		Combined effect	
	Treatment/ Plant part	Co		EE2		Co + EE2		Co + EE2		Co + EE2		Co + EE2	
	Parameter	Shoots	Roots	Shoots	Roots	Shoots	Roots	Shoots	Roots	Shoots	Roots	Shoots	Roots
Biometry	Size	—	—	↑	—	—	—	—	—	↓	—	-	○
	Biomass	↓	↓	—	—	—	—	↑	↑	—	—	-	-
Biochemical	MDA levels	—	↑	—	↑	↑	↑	—	—	—	—	+	○
	H_2O_2 levels	↑	↑	—	—	↑	↑	↑	—	↑	↑	+	○
	Pro levels	—	—	—	—	—	↓	—	—	—	—	○	+
	GSH levels	—	—	—	↓	↑	—	↑	—	↑	↑	+	-
	Total ascorbate levels	↑	—	—	—	↑	↑	↑	—	↑	↑	+	+
	AsA levels	—	↑	—	—	↑	↑	↑	—	↑	↑	+	○
	DHA levels	—	—	—	—	↑	-	↑	—	↑	—	+	○
	AsA/total	—	↑	—	—	↓	↑	—	—	—	↑	+	○
	DHA/total	—	↓	—	—	↑	↓	—	—	—	↓	+	○
	AsA/DHA	—	↑	—	—	—	↑	—	—	—	↑	○	○
	SOD activity	↓	—	—	—	—	—	—	—	—	—	-	○
	APX activity	—	—	↓	—	↓	—	↓	—	—	—	○	○
	GR activity	—	—	↓	—	↓	↑	↓	—	—	↑	○	+
	GST activity	—	—	↑	—	↑	—	—	—	—	—	○	○
Molecular	*MT1* expression	—	↑	↑	↑	↓↓	↑	↓↓	↓	↓↓	—	-	-
	MT2 expression	↓	↑	↓	↓	—	—	↑	↓	↑	—	-	-
	MT4 expression	—	↑	—	↑	↓↓	—	↓↓	↓	↓↓	↓	-	-
	GR_{plast} expression	↑	↑	—	↑	↓	↑	↓	—	↓	—	-	○
	GSTU expression	↑	—	↑	—	↓	↓	↓	↓	↓	↓	-	-
	PCS expression	↑	—	—	↓	↓↓	↓	↓↓	↓	↓↓	↓	-	-
	γ-ECS expression	↑	—	—	↓	↓↓	↓	↓↓	↓	↓↓	↓	-	-